

MEASURED METALLICITIES AT THE SITES OF NEARBY BROAD-LINED TYPE Ic SUPERNOVAE AND IMPLICATIONS FOR THE SUPERNOVAE GAMMA-RAY BURST CONNECTION*

M. MODJAZ^{1,2}, L. KEWLEY^{3,8}, R. P. KIRSHNER¹, K. Z. STANEK⁴, P. CHALLIS¹, P. M. GARNAVICH⁵, J. E. GREENE^{6,8}, P. L. KELLY⁷,
AND J. L. PRIETO⁵

¹ Harvard-Smithsonian Center for Astrophysics, 60 Garden Street, Cambridge, MA, 02138, USA; mmodjaz@cfa.harvard.edu, kirshner@cfa.harvard.edu, and pchallis@cfa.harvard.edu

² Department of Astronomy, University of California, Berkeley, 601 Campbell Hall, Berkeley, CA 94720, USA; mmodjaz@astro.berkeley.edu

³ University of Hawaii, 2680 Woodlawn Drive, Honolulu, HI 96822, USA; kewley@ifa.hawaii.edu

⁴ Department of Astronomy, The Ohio State University, Columbus, OH 43210, USA; kstanek@astronomy.ohio-state.edu

⁵ Department of Physics, 225 Nieuwland Science Hall, University of Notre Dame, Notre Dame, IN 46556, USA; pgarnavi@nd.edu, prieto@astronomy.ohio-state.edu

⁶ Department of Astrophysical Sciences, Princeton University, Peyton Hall, Ivy Lane, Princeton, NJ 08544-1001, USA; jgreene@astro.princeton.edu

⁷ Kavli Institute for Particle Astrophysics and Cosmology, 2575 Sand Hill Road, MS 29, Menlo Park, CA 94025, USA

Received 2007 January 12; accepted 2007 December 18; published 2008 March 4

ABSTRACT

We compare the chemical abundances at the sites of 12 nearby ($z < 0.14$) Type Ic supernovae (SN Ic) that showed broad lines, but had no observed gamma-ray burst (GRB), with the chemical abundances in five nearby ($z < 0.25$) galaxies at the sites of GRBs where broad-lined SN Ic were seen after the fireball had faded. It has previously been noted that GRB hosts are low in luminosity and low in their metal abundances. If low metallicity is sufficient to force the evolution of massive stars to end their lives as GRBs with an accompanying broad-lined SN Ic, then we would expect higher metal abundances for the broad-lined SN Ic that have no detected GRBs. This is what we observe, and this trend is independent of the choice of metallicity calibration we adopt and the mode of SN survey that found the broad-lined SN Ic. A unique feature of this analysis is that we present new spectra of the host galaxies and analyze all measurements of both samples in the same set of methods, using the galaxy emission-line measurements corrected for extinction and stellar absorption, via independent metallicity diagnostics of Kewley & Dopita, McGaugh, and Pettini & Pagel. In our small sample, the boundary between galaxies that have GRBs accompanying their broad-lined SN Ic and those that have broad-lined SN Ic without GRBs lies at an oxygen abundance of $12 + \log(\text{O}/\text{H})_{\text{KD02}} \sim 8.5$, which corresponds to $0.2\text{--}0.6 Z_{\odot}$ depending on the adopted metallicity scale and solar abundance value. Even when we limit the comparison to SN Ic that were found in untargeted supernova surveys, the environment of every broad-lined SN Ic that had no GRB is more metal rich than the site of any broad-lined SN Ic where a GRB was detected.

Key words: galaxies: abundances – galaxies: distances and redshifts – gamma rays: bursts – supernovae: general

Online-only material: color figures

1. INTRODUCTION

We seek clues to the stellar origin of long-duration gamma-ray bursts (GRBs) by comparing the chemical abundances at the sites of the broad-lined Type Ic supernovae (SN Ic) that accompany some GRBs with the broad-lined SN Ic that have no observed GRBs. In nearby GRBs, after the afterglow has faded, if the spectrum of the underlying event is observed, it is that of a broad-lined SN Ic (e.g., Galama et al. 1998; Stanek et al. 2003; Hjorth et al. 2003; Modjaz et al. 2006). These are supernovae whose spectra show no trace of hydrogen or of helium and whose line widths approach $30,000 \text{ km s}^{-1}$ (e.g., Galama et al. 1998; Patat et al. 2001; Pian et al. 2006). SN Ic with broad lines are also seen without an accompanying GRB. We have studied these objects, and their hosts, to try to learn more about the conditions that lead a massive star to have the special kind of core collapse that leads to the formation of a jet and a GRB (see Woosley & Bloom 2006 for a review).

Some models of core collapse in massive stars produced to match these spectra have large kinetic energies ($E_K > 10^{52}$ erg; Iwamoto et al. 1998; Mazzali et al. 2003), and thus have led to

the use of the term “Hypernova.” However, since the computed E_K are model dependent (Maeda et al. 2006) and for some cases not necessarily larger than those of normal core-collapse SN (Mazzali et al. 2006a), we prefer to use names that reflect the directly observed properties, without any implication on the overall energy budget for the event. Thus, we call them “broad-lined SN Ic,” abbreviated as “SN Ic (broad),” and for comparison, we henceforth call and abbreviate broad-lined SN Ic associated with GRBs as “SN Ic (broad & GRB)” (see Section 2.2).

A number of studies have been conducted on the environments of GRBs to help constrain their progenitors. Observations of host galaxies of nearby GRBs ($z < 0.25$) indicate that they are faint, blue, star-forming galaxies with low metallicities⁹ (Prochaska et al. 2004; Sollerman et al. 2005; Modjaz et al. 2006; Stanek et al. 2006; Thoene et al. 2007; Wiersema et al. 2007; Margutti et al. 2007). Studies of GRB hosts at cosmological distances draw a similar conclusion (Fruchter et al. 1999, 2006; Le Floch et al. 2003; Fynbo et al. 2003): GRB hosts tend to be consistently dimmer and more irregular than galaxies that host core-collapse SN at comparable redshifts and GRBs appear concentrated in the highest surface brightness areas of their blue hosts. In addition,

* This paper includes data gathered with the MMT Observatory, a joint facility of the Smithsonian Institution and the University of Arizona, and with the 6.5 m Magellan Telescopes located at Las Campanas Observatory, Chile.

⁸ Hubble Fellow.

⁹ Here we refer to the term “metallicity” as represented by the gas-phase oxygen abundance and use these two terms interchangeably. See Section 4.2 for details.

Kewley et al. (2007) and Brown et al. (2008) have discovered a number of extremely metal-poor galaxies that do not follow the regular galaxy luminosity–metallicity (hereafter L – Z) relationship (Garnett 2002; Tremonti et al. 2004), just like the nearby GRB host galaxies. For the same M_B , they are more metal poor than dwarf irregular galaxies, normal blue galaxies, and normal star-forming galaxies (see also Figure 3 in Savaglio et al. 2006 for a similar trend for hosts of higher z GRBs). Thus, based on observations, Fruchter et al. (2006) and Stanek et al. (2006) argue that low metallicity is required for GRB progenitors, in line with theoretical GRB models that suggest rapidly rotating massive stars at low metallicity (Hirschi et al. 2005; Yoon & Langer 2005; Woosley & Heger 2006; Langer & Norman 2006) as likely progenitors. Low metallicity seems to be a promising route for some stars to avoid losing angular momentum from mass loss (Vink & de Koter 2005; Crowther & Hadfield 2006). High angular momentum and a massive core are key ingredients for producing a GRB jet. If the abundances in the star are low enough, then hydrogen and helium can mix into the burning zones of the star, leading to a star with low hydrogen and helium abundances and a large core mass just before explosion (Hirschi et al. 2005; Yoon & Langer 2005; Woosley & Heger 2006; Langer & Norman 2006). This mechanism for producing a GRB seems plausible for producing a broad-lined SN Ic at the same time, as observed.

However, the SN Ic that are observed to erupt without a GRB may provide essential clues to complete this picture. If low metal abundance always accompanies jet formation in the core collapse of massive stars, then broad-lined SN Ic intrinsically without GRBs should be found in metal-rich environments. This is the hypothesis we test here, using the available list of broad-lined SN Ic and our own uniform determinations of the local metal abundance. Though the present sample is small, it is intriguing, and we look forward to future discoveries that can test the conclusions presented here.

After the discovery of SN 1997ef, around 15 additional broad-lined SN Ic were discovered, which have spectroscopic properties similar to the broad-lined SN Ic–GRBs when studied in detail. Studying the full class of broad-lined SN Ic may help us understand the mechanism for producing jet-driven explosions. Since these SN are more frequent than nearby GRBs, we may gain clues more rapidly than waiting for the detection of the next nearby GRB. Three of the nearby SN–GRBs have gamma-ray energies 2–4 orders of magnitude lower compared to cosmological ones and might belong to a different class of GRBs that is much more frequent (by a factor of 10^2 – 10^3), but not observable at high z due to their low gamma-ray energies (Cobb et al. 2006; Liang et al. 2007; Guetta & Della Valle 2007). Thus, it is still worthwhile to investigate the specific conditions which give rise to low- z GRBs, even if those insights cannot be directly applied to cosmological, high-energy GRBs.

Previous work has investigated the metallicity dependence of GRBs; however, these studies (Wolf & Podsiadlowski 2007) are based on indirect measures of galaxy metallicity. Not only do these relations contain significant scatter (Tremonti et al. 2004), but there is evidence that the L – Z relation is no longer linear at very low metallicity for certain galaxies (Kewley et al. 2007; Brown et al. 2008; Kniazev et al. 2003). In this paper, we present the *measured* metallicities of a statistically significant sample of broad-lined SN Ic environments, derived in the same fashion, with which the SN–GRB host sample should be and will be compared. This study constitutes the first of its kind for core-collapse SN.

Table 1

Sample of Broad-Lined SN Ic Associated with GRBs and their Hosts

GRB/SN name	Host galaxy	Hubble type	Redshift z	References
GRB 980425/SN 1998bw	ESO 184-G82	SB	0.0085	1, 2
GRB 031203/SN 2003lw	Anon.	...	0.1055	3, 4
XRF 020903	Anon.	...	0.2500	5, 6
GRB/XRF 060218/SN 2006aj	Anon.	...	0.0335	6, 7
GRB 030329/SN 2003dh	Anon.	...	0.1685	1, 8, 9

Notes.

References. (1) Sollerman et al. (2005); (2) Hammer et al. (2006); (3) Prochaska et al. (2004); (4) Margutti et al. (2007); (5) Bersier et al. (2006); (6) Modjaz et al. (2006); (7) Wiersema et al. (2007); (8) Gorosabel et al. (2005); (9) Thoene et al. (2007).

In Section 2.1 we summarize the sample of broad-lined SN Ic with GRBs from the literature, while in Section 2.2 we introduce our sample of local broad-lined SN Ic and their hosts and discuss the role of selection effects in Section 2.3. We then present the spectroscopic observations in Section 3 and derive galaxy parameters in Section 4. We discuss our results and their implications in Section 5 and summarize in Section 6. In this paper, we adopt the following values of the cosmological parameters: $H_0 = 70 \text{ km s}^{-1} \text{ Mpc}^{-1}$, $\Omega_m = 0.3$, and $\Omega_\Lambda = 0.7$.

2. SN HOST-GALAXY SAMPLES

2.1. Sample of Broad-Lined SN Ic with GRBs and their Hosts

There are currently four nearby secure cases of direct SN–GRB associations: the temporal and spatial coincidence between SN 1998bw and GRB 980425 (Galama et al. 1998) and the metamorphosis of the GRB afterglow spectra into that of a supernovae for the following SN–GRBs: GRB 030329/SN 2003dh (Stanek et al. 2003; Hjorth et al. 2003; Matheson et al. 2003); GRB 031203/SN 2003lw (Malesani et al. 2004; Mazzali et al. 2006b); GRB/XRF 060218/SN 2006aj (Modjaz et al. 2006; Pian et al. 2006; Mazzali et al. 2006a; Campana et al. 2006; Mirabal et al. 2006; Sollerman et al. 2006; Cobb et al. 2006). We also include the host of XRF 020903, that had a clear supernova signature in its light curve (Bersier et al. 2006) and in its afterglow spectrum (Soderberg et al. 2005), but we do note that this SN confirmation has a lower degree of certainty than the other GRB–SN associations.¹⁰ The nearby SN connected with GRBs have been well observed and in all cases their host-galaxy properties and emission-line fluxes measured. We list in Table 1 the SN–GRB sample, and the references include published host-galaxy emission-line fluxes which we directly use when deriving metallicities in Section 4.2. While there are certain conditions that might favor detecting certain SN spectroscopically in GRB afterglows (e.g., good burst localization, weak GRB afterglow, low redshift), a detailed analysis is beyond the scope of this paper, and we refer the reader to the discussion in Woosley & Bloom (2006).

2.2. Sample of Broad-Lined SN Ic and their Hosts

In our study, we include the host galaxies of the four broad-lined SN Ic which are well documented in the literature and whose properties have been observed and modeled: SN

¹⁰ There is some evidence of spectroscopically confirmed supernovae for other GRBs, although with less confidence (Della Valle et al. 2003; see Woosley & Bloom 2006 for a full list).

Table 2
Sample of Broad-Lined SN Ic without Observed GRB and their Hosts

SN name	Host galaxy	Hubble type	Redshift z	R.A. offset ($''$) ^a	Decl. offset ($''$) ^a	References	Disc type ^b
SN 1997dq	NGC 3810	SA(rs)c	0.0033	43.W	29.N	1, 2	T
SN 1997ef	UGC 4107	SA(rs)c	0.0117	10.E	20.S	3, 4	T
SN 1998ey	NGC 7080	SB(r)b	0.0161	18.W	20.N	5, 6	T
SN 2002ap	M 74	SA(s)c	0.0022	258.W	108.S	7, 8	T
SN 2003bg	MCG-05-10-15	SB(s)c	0.0044	16.W	25.S	9, 10	T
SN 2003jd	MCG-01-59-21	SAB(s)m	0.0188	8.E	8.S	11, 12	T
SN 2005da	UGC 11301	Sc	0.0150	108.W	35.N	13, 14	T
SN 2005fk	J211520.09–002300.3	...	0.2650	4.W	2.N	15	Non-T
SN 2005nb	UGC 07230	SB(s)d-pec	0.0238	1.5W	5.N	16	Non-T
SN 2005kr	J030829.66+005320.1	...	0.1345	0.0E	0.1N	17	Non-T
SN 2005ks	J213756.52–000157.7	...	0.0987	0.0E	0.8N	17	Non-T
SN 2005kz	MCG+08-34-032	Sc;LINER	0.0270	16.W	10.N	18, 19	T
SN 2006nx	J033330.43–004038.0	...	0.1370	0.2E	0.2S	20	Non-T
SN 2006qk	J222532.38+000914.9	...	0.0584	0.0E	0.2N	21	Non-T
SN 2007l	J115913.13–013616.1	...	0.0216	0.8E	0.8S	22, 23	Non-T

Notes.

^a Offset from the center of host galaxy as listed in discovery IAUCs or as derived by comparing SN and host-galaxy coordinates.

^b Discovery type: T: SN host galaxy was targeted; Non-T: SN host galaxy was not targeted.

References. (1) Nakano et al. (1997); (2) Matheson et al. (2001); (3) Hu et al. (1997b); (4) Hu et al. (1997a); (5) Schwartz (1998); (6) Garnavich et al. (1998); (7) Nakano et al. (2002); (8) Kinugasa et al. (2002); (9) Chassagne (2003); (10) Filippenko & Chornock (2003); (11) Burket et al. (2003); (12) Filippenko et al. (2003); (13) Lee & Li (2005); (14) Modjaz et al. (2005); (15) Barentine et al. (2005a); (16) Quimby et al. (2006); (17) Barentine et al. (2005b); (18) Puckett et al. (2005); (19) Filippenko et al. (2005); (20) Bassett et al. (2006a); (21) Bassett et al. (2006b); (22) Lee & Li (2007); (23) Blondin et al. (2007).

1997ef and SN 1997dq (Iwamoto et al. 2000), SN 2002ap (e.g., Gal-Yam et al. 2002; Mazzali et al. 2002; Foley et al. 2003), and SN 2003jd (Mazzali et al. 2005). We also include SN 2003bg, which was classified as a broad-lined SN Ic (Filippenko & Chornock 2003). It then developed P Cygni absorption features of hydrogen (Hamuy et al. 2003), but did not display any H emission in late-time spectra as expected in Type II SN (M. Hamuy et al. 2008, in preparation). Thus, we count SN 2003bg as a broad-lined SN Ic, with some hydrogen possibly due to interstellar medium (ISM) interactions (Soderberg et al. 2006a). In addition, we searched the International Astronomical Union Circulars (IAUCs)¹¹ for announcements of broad-lined SN Ic. We list the sample for which we obtained data in Table 2. Column 1 indicates the supernova, Column 2 its host galaxy, Columns 3 and 4 the Hubble type (in the RC3 system) and redshift of the host galaxy as listed in the NASA/IPAC Extragalactic Database (NED) or as determined by the Sloan Digital Sky Survey (SDSS) pipeline for SDSS galaxies. Columns 5 and 6 list the offsets in right ascension (R.A.) and declination (Decl.) of the SN from the host-galaxy nucleus. The discovery IAUC and the circulars with the spectroscopic SN identification are listed in Column 7. In Column 8 we list the fashion in which the broad-lined SN Ic were discovered: “T” stands for cases where the SN host galaxy was targeted, while “Non-T” SN hosts were not. The latter group consists of SN that were found in rolling, wide-field and non-targeted searches, or in background galaxies of fields with targeted galaxies. The discovery method is important for assessing the significance of selection effects in our sample. We discuss the implications and significance of Column 8 in the following section in more detail.

2.3. Controlling for Selection Effects

GRBs and SN are usually found in dramatically different ways. GRBs are discovered in wide-field, nearly all-sky searches with gamma-ray satellites such as BATSE, *HETE* or *Swift*, whose afterglow studies have lead to the discovery of SN in certain GRBs.

Most traditional searches for nearby SN, however, are galaxy-targeted searches. The successful Lick Observatory SN Search (LOSS, Filippenko et al. 2001) and many amateur SN searches possess a relatively small field-of-view (FOV, 8.7×8.7 for LOSS) and have a database of galaxies that they monitor nightly. Thus, they include well-known and inevitably, more luminous galaxies (e.g., Li et al. 2001; Gallagher et al. 2005; Mannucci et al. 2005). In particular, the LOSS database of 10,341 galaxies with measured M_B -values has a mean (median) value at the galaxy magnitude of $M_B = -19.9$ ($M_B = -20.1$) mag with a standard deviation of 1.3 mag (J. Leaman 2007, private communication). We are aware that selection effects can be introduced by different methods of discovery. This is why we have worked hard to include SN that were found in host galaxies that had not been targeted for search. We believe they provide a better match to the host galaxies that are selected by the appearance of a GRB.

Those six broad-lined SN were found either via the Sloan Digital Sky Survey-II (SDSS-II) SN survey,¹² or via the Texas SN Survey¹³ (Quimby 2006) that are both rolling searches with a large field of view (FOV) (1–3 square degrees) and thus can be considered galaxy-impartial surveys. In other cases, they were found in background galaxies of LOSS target fields (W. Li 2007, private communication), and thus can also be considered SN with non-targeted host galaxies. Assuming that

¹¹ <http://cfa-www.harvard.edu/iau/cbat.html>.

¹² <http://www.sdss.org/supernova/aboutsprnova.html>.

¹³ <http://grad40.as.utexas.edu/quimby/tss/index.html>.

the sample of SDSS star-forming galaxies from Tremonti et al. (2004) is representative of the galaxies surveyed by the SDSS-II SN search, the mean (median) galaxy luminosity is $M_B \sim -19.0$ ($M_B \sim -19.1$) mag, i.e., one magnitude fainter than the mean value for the LOSS sample. Moreover, the untargeted searches employ image-subtraction techniques and thus are sensitive to SN occurring at the center of galaxies.

For completeness, we analyze and discuss spectra of all SN Ic (broad). But when directly comparing to the sample of SN Ic (broad & GRB), we only include SN Ic (broad) found in the same, non-targeted fashion in order to minimize discovery selection effects. The sample size of SN Ic (broad) that are free of galaxy-selection effects is comparable to that of SN-GRBs.

2.4. GRB Non-Detections

Here we investigate whether the broad-lined SN Ic in Table 2 had a detected GRB.

Wang & Wheeler (1998) suggested that SN 1997ef and SN 1997dq were associated with GRB 971115 and GRB 971013, respectively. However, their spatial and, more stringently, their temporal concurrences are much weaker than for GRB 980425/SN 1998bw (for detailed discussion see Li 2006 and Woosley & Bloom 2006). Thus, claims of GRB associations for SN 1997ef and SN 1997dq are much less compelling than those for cases such as GRB 980425/SN 1998bw. Furthermore, no GRB was found to be associated with SN 2002ap (Hurley et al. 2002).

Mazzali et al. (2005) have argued for an off-axis GRB in SN 2003jd via late-time spectral signatures of an aspherical explosion seen from along the equatorial plane. On the other hand, Soderberg et al. (2006b) present a search for late-time radio emission of a sample of 68 SN Ib/c and argue against a GRB connection for SN 2003jd, as well as for all non-SDSS SN of our sample (except SN 2005nb). We discuss if SN 2003jd had an off-axis GRB in more detail in Section 5.2, along with the broader question of viewing angle effects.

For the rest of the broad-lined SN Ic in our sample, we consulted the GRB localizations¹⁴ and did not find any significant spatial (within ± 2 deg) nor temporal (within ± 20 days) concurrences. Thus, we assume that no GRBs were observed for those broad-lined SN Ic.

3. SPECTROSCOPIC OBSERVATIONS

3.1. CfA Data

Eight of the total of 17 host-galaxy spectra were obtained with the 6.5 m Clay Telescope of the Magellan Observatory located at Las Campanas Observatory (LCO), with the 6.5 m MMT and the 1.5 m Tillinghast telescope at the Fred Lawrence Whipple Observatory (FLWO). The spectrographs utilized were the LDSS-3 (Mulchaey & Gladders 2005) at LCO, the Blue Channel (Schmidt et al. 1989) at the MMT, and FAST (Fabricant et al. 1998) at the FLWO 1.5 m telescope. All optical spectra were reduced and calibrated employing standard techniques (see e.g., Modjaz et al. 2001) in IRAF¹⁵ and our own IDL routines for flux calibration.

Extraction of the spectra was done using the optimal weighting algorithm (Horne 1986), and wavelength calibration was

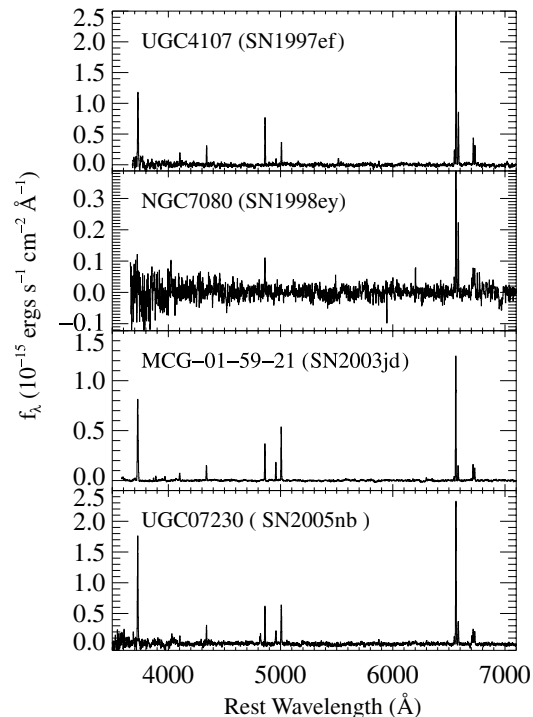


Figure 1. Host-galaxy spectra of four local broad-lined SN Ic at the SN position, with the SN spectrum subtracted. The host-galaxy names and corresponding SN are given in the figure. They were de-redshifted using values listed in Table 2. See Section 3 and Table 3 for details.

accomplished with HeNeAr lamps taken at the position of the targets. Small-scale adjustments derived from night-sky lines in the observed frames were also applied. The spectra were always taken at or near the parallactic angle (Filippenko 1982) and at low airmass. Comparison of $(B - V)$ colors of SN derived from spectroscopy using the same telescopes and instruments yields consistency with SN photometry at the 5% level (Matheson et al. 2007); thus, we are confident that our relative flux calibration is accurate to $\sim 5\%$ across 4000–6500 Å and most likely across the rest of the covered wavelength range. Telluric lines were removed following a procedure similar to that of Wade & Horne (1988) and Matheson et al. (2000). The final flux calibrations were derived from observations of spectrophotometric standard stars.

In Table 3 we list the details of our spectroscopic observations. Exposures over multiple nights were averaged for SN 1997ef and SN 2003jd to increase the signal-to-noise ratio (S/N). In four cases (UGC 4107, NGC 7080, MCG-01-59-21, UGC7230, i.e. hosts of SN 1997ef, 1998ey, 2003jd and 2005nb, respectively), a spline fit to the continuum was subtracted, in order to eliminate the supernova contribution. This procedure is adequate to study the emission-line component of the host galaxy at the position of the SN. Since the SN features are very broad ($\sim 10,000$ – $30,000$ km s⁻¹) compared to the nebular galaxy emission lines (200 – 400 km s⁻¹), there are no significant errors ($\lesssim 5\%$) in the emission-line measurements due to interpolation errors. Figure 1 shows the emission-line spectra of four host galaxies at the position of the SN, with the SN spectrum subtracted. In Figure 2, we present central spectra obtained with Clay+LDSS3 and FLWO1.5m+FAST.

¹⁴ See <http://www.mpe.mpg.de/~jcg/grbgen.html>.

¹⁵ IRAF is distributed by the National Optical Astronomy Observatories, which are operated by the Association of Universities for Research in Astronomy, Inc., under cooperative agreement with the National Science Foundation.

Table 3
Journal of Spectroscopic Observations of Host Galaxies of Broad-Lined SN Ic

SN	UT date	Julian day −2,450,000	Telescope ^a	Observed range (Å)	Resolution (Å)	Airmass ^b	Slit (″)	Exp. (s)	Spectrum-type ^c
SN 1997ef	1997-11-26.39	778.89	FLWO	3720–7540	7.0	1.12	3.00	1200	SN
SN 1997ef	1997-11-28.52	781.02	FLWO	3720–7540	7.0	1.11	3.00	1200	SN
SN 1997ef	1997-11-29.42	781.92	FLWO	3720–7540	7.0	1.06	3.00	1200	SN
SN 1997ef	1997-11-30.34	782.84	FLWO	3720–7540	7.0	1.19	3.00	1200	SN
SN 1997ef	1997-12-01.33	783.83	FLWO	3720–7540	7.0	1.22	3.00	1200	SN
SN 1997ef	1997-12-04.34	786.84	FLWO	3720–7540	7.0	1.17	3.00	1200	SN
SN 1997ef	1997-12-05.31	787.81	FLWO	3720–7540	7.0	1.26	3.00	1200	SN
SN 1997ef	1997-12-06.33	788.83	FLWO	3720–7540	7.0	1.17	3.00	1200	SN
SN 1998ey	1998-12-12.14	1159.64	FLWO	3720–7540	7.0	1.52	3.00	1200	SN
SN 2002ap	2006-11-20.23	4059.73	FLWO	3479–7417	7.0	1.04	3.00	600	Central
SN 2003bg	2006-09-21.0	3999.50	LCO	3800–10,000	7.0	1.00	1.25	5 × 600	Central
SN 2003jd	2003-12-19.13	2992.63	MMT	3650–8850	8.0	1.49	1.00	900	SN
SN 2003jd	2003-12-20.7	2993.57	MMT	3620–8830	8.0	1.28	1.00	3 × 1200	SN
SN 2005da	2006-10-25.08	4033.58	MMT	3340–8521	8.0	1.25	2.00	600	Central
SN 2005fk	2006-09-21.0	3999.50	LCO	3800–10,000	7.0	1.21	3.00	4 × 1800	Central
SN 2005kr	2006-09-21.0	3999.50	LCO	3800–10,000	7.0	1.38	1.25	3 × 1800	SN, Central
SN 2005kz	2006-10-25.11	4033.61	MMT	3340–8521	8.0	1.19	2.00	600	Central
SN 2005nb	2006-01-09.51	3745.01	FLWO	3500–7410	7.0	1.04	3.00	1800	SN
SN 2006nx	2006-12-13.0	4082.50	LCO	4060–10,600	7.0	1.40	1.00	2 × 1200	SN, Central

Notes.

^a FLWO, Tillinghast 1.5 m/FAST; LCO, 6.5 m Clay Telescope of the Magellan Observatory located at Las Campanas Observatory/LDSS-3; MMT, 6.5 m MMT/Bluechannel.

^b Airmass at the middle of the set of observations.

^c SN: spectrum at the position of the SN; Central: spectrum of the central part of the host galaxy.

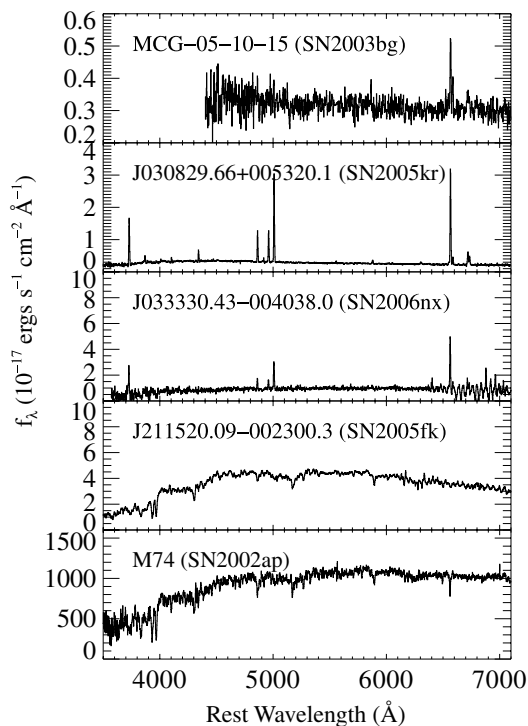


Figure 2. Central host-galaxy spectra of five local broad-lined SN Ic observed with Magellan+LDSS3 and the FLWO1.5m+FAST. The host-galaxy names and corresponding SN are given in the figure. They were de-redshifted using values listed in Table 2. See Section 3 and Table 3 for details.

3.2. Archival Data

Five central host-galaxy spectra were taken from the Fifth Data Release of the SDSS (York et al. 2000; Stoughton et al.

2002).¹⁶ The spectra were acquired with the SDSS 2.5 m telescope using fiber-fed spectrographs, with the fiber subtending a diameter of 3″ (for a full discussion of aperture effects see Tremonti et al. 2004). Exposure times had been chosen to lead to an S/N of at least 4 at $g = 20.2$ mag and range from 2160 to 5500 s. The central spectra have an instrumental resolution of $R = \frac{\lambda}{\Delta\lambda} \sim 1800$ (i.e., FWHM ~ 2.4 Å at 5000 Å) and span 3800–9200 Å in observed wavelength. The SDSS spectroscopic pipeline performed the basic reductions, including extraction, flux and wavelength calibrations and removal of atmospheric bands. The spectra are shown in Figure 3, with and without stellar contribution (see Section 3.3 for more details).

The central spectrum of SN 2003jd (Figure 4) was retrieved from the 6dF Galaxy Survey DR2¹⁷ (Jones et al. 2004; Jones et al. 2005). The spectrum was acquired with the Six-Degree Field multi-object fiber spectroscopy facility (with fibers 6.7″ in diameter) in two observations using separate V and R gratings, that combined result in an instrumental resolution of $R = \frac{\lambda}{\Delta\lambda} \sim 1000$, range from 4000 to 7500 Å, with typical S/N of ~ 10 per pixel.

3.3. Emission-Line Measurements

The focus of this paper is the analysis of the nebular emission lines of broad-lined SN Ic host galaxies. However, for

¹⁶ We used the Princeton spectral reductions (<http://spectro.princeton.edu/>). We note that for two of the five SDSS galaxy spectra, the Princeton reductions give fluxes larger by a factor of 2 than the official data release at <http://cas.sdss.org/dr5/en/tools/explore/>. This difference is merely due to a different flux normalization convention between the SDSS database (spectrum normalized to the fiber magnitude) and the Princeton database (spectrum normalized to the point-spread function (PSF) magnitude), and does not imply different reduction steps (J. Frieman 2007, private communication). Nevertheless, this normalization convention does not change our metallicity determinations as they are based on line flux ratios.

¹⁷ See <http://www-wfau.roe.ac.uk/6dFGS/>.

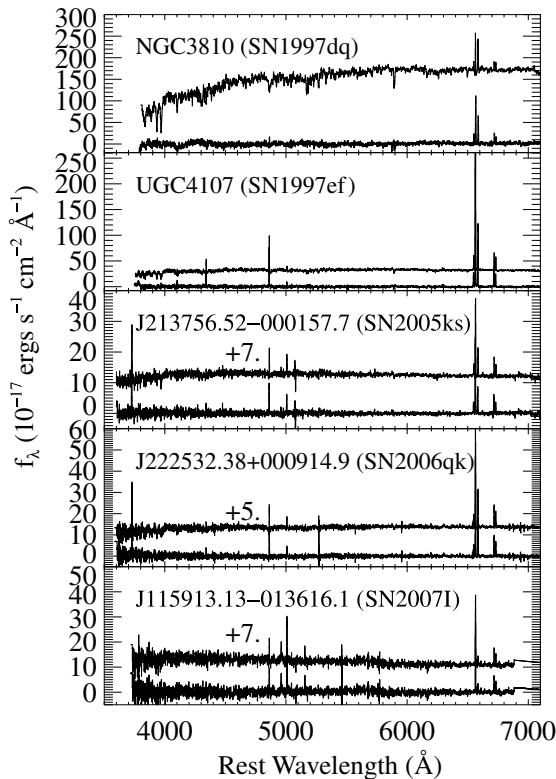


Figure 3. Central host-galaxy spectra of five local broad-lined SN Ic taken from the SDSS database plotted with (top) and without (bottom) stellar contribution (see Section 3.3 for details). Any offsets by an additive constant done for clarity purposes are indicated. Note that weak nebular emission lines become more apparent in stellar-continuum-subtracted spectra. The host-galaxy names and corresponding SN are given in the figure. They were de-redshifted using values listed in Table 2. See the text for details.

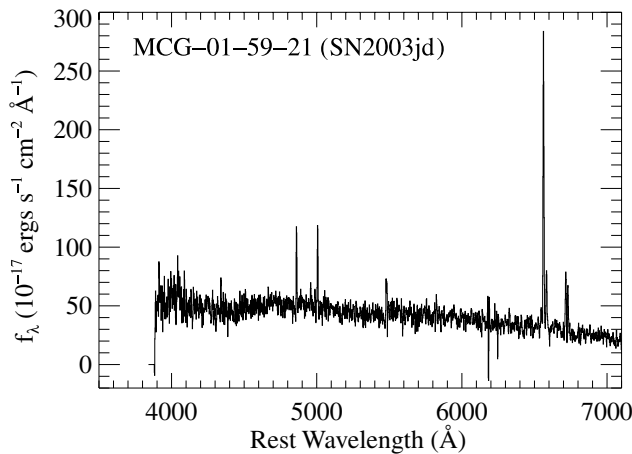


Figure 4. Central host-galaxy spectra of SN 2003jd, taken from the 6dF Galaxy Survey, de-redshifted using the value listed in Table 2. See Section 3.

spectra of galaxy nuclei, the presence of stellar *absorption* features may contaminate the emission components, especially the Balmer lines (e.g., Tremonti et al. 2004; Moustakas & Kennicutt 2006a). This is not a concern for spectra of H II regions near or at the position of the SN, as there the light-weighted emission is contributed foremost by hotter stars with weak Balmer

lines. In our sample of nine central spectra, we encountered seven central spectra with significant stellar features. To remove the starlight we utilize the method of stellar template subtraction (see Ho 2004 for a full discussion of the different techniques); in particular, we employ the standard principal component analysis (PCA) technique developed by Hao et al. (2005) for use on SDSS data (see also Greene & Ho 2004). Using an approach pioneered by Bromley et al. (1998) for the Las Campanas Redshift Survey (see also Connolly et al. 1995), we employ the methods of Hao et al. (2005) to use a library of SDSS spectra for absorption-line galaxies that is transformed into an orthogonal basis of “eigenspectra” spanning the variance in the sample. We model the absorption and continuum part of the input galaxy spectrum as a linear combination of eight eigenspectra plus an additional A-star component. The PCA method is especially powerful since it does not assume single-metallicity populations, uses the homogeneous survey data of SDSS as templates, need not include the galaxy velocity dispersion and spans a large range in galaxy properties with a very small number of components. In Figure 3, we plot the affected original spectra (top) and spectra after subtracting the modeled stellar continuum (bottom): the SDSS spectra of NGC 3810, UGC 4107, SDSS J213756.52–000157.7, SDSS J222532.38+000914.9, and SDSS J115913.13–013616.0, i.e., the host galaxies of SN 1997dq, 1997ef, 2005ks, 2006qk, and 2007I, respectively. Thus, we arrive at emission-line spectra.

For M 74, UGC 11301, and SDSS J211520.09–002300.3, the host galaxies of SN 2002ap, 2005da, and 2005fk, respectively, we are unable to recover any emission lines in their central regions, due to the low surface brightness or absence of H II regions. Since M 74 is a nearby, well-observed star-forming spiral galaxy, we consult the literature for the emission-line fluxes of its H II regions as a function of radius (see Section 4.2). For the hosts of SN 2005da and 2005fk, we are not able to measure emission-line-based metallicities and refrain from using Lick indices, as systematic offsets plague different metallicity methods. The low surface brightness or absence of H II regions implies little instantaneous (i.e., in the last ~ 3 million years) star formation for these galaxies.

After properly correcting all spectra for their recession velocities (as listed in Table 2), we measure optical emission-line properties by fitting Gaussians to the individual spectral lines via the *splot* routine in IRAF. The emission-line fluxes and their statistical errors are given in Tables 4 and 5. For the derivation of the statistical errors, we follow Pérez-Montero & Díaz (2003) and use spectra before continuum subtraction to measure their noise properties. The total errors are computed by adding the statistical errors and the 5% flux calibration error in quadrature.

In the subsequent analysis, we correct the line fluxes for Galactic reddening, according to Schlegel et al. (1998), and for intrinsic reddening by using the observed Balmer decrement, if H β emission line is detected. We assume case B recombination and thus, the standard value of 2.86 as the intrinsic H α /H β ratio (Osterbrock 1989), and apply the standard Galactic reddening law with $R_V = 3.1$ (Cardelli et al. 1989). Tables 6 and 7 list in Column 9 the color excess due to the SN host galaxy $E(B - V)_{\text{Host}}$ derived from the observed Balmer decrement, a robust indicator of the amount of dust (e.g., Calzetti et al. 1994; Kewley et al. 2002; Moustakas & Kennicutt 2006b).

Table 4
Central Galaxy Emission-Line Measurements

Emission line	SN 1997dq	SN 1997ef	SN 2003bg	SN 2003jd	SN 2005kr ^a	SN 2005ks ^a	SN 2006nx ^a	SN 2006qk ^a	SN 2007l ^a
[O II] $\lambda\lambda 3726, 29$	13.7 \pm 1.4	170 \pm 19	15.2 \pm 2.5	102 \pm 14	...
H δ $\lambda 4101$	1.23 \pm 0.16
H γ $\lambda 4340$...	67.3 \pm 8.4	...	1421 \pm 330	3.04 \pm 0.32	15.7 \pm 3.4	...
H β $\lambda 4861$	68 \pm 10	239 \pm 25	...	4620 \pm 530	8.20 \pm 0.83	69.6 \pm 7.3	6.9 \pm 1.1	43.7 \pm 5.0	28.7 \pm 2.9
[O III] $\lambda 4959$	940 \pm 250	8.40 \pm 0.85	13.7 \pm 2.0	6.87 \pm 0.94	...	11.9 \pm 2.9
[O III] $\lambda 5007$...	28.5 \pm 5.7	...	4300 \pm 630	24.3 \pm 2.4	51.2 \pm 5.5	20.9 \pm 2.2	15.3 \pm 2.6	57.2 \pm 7.1
[He I] $\lambda 5876$	1.15 \pm 0.14
[O I] $\lambda 6300$...	20.5 \pm 3.5	...	720 \pm 310	1.03 \pm 0.13	9.5 \pm 1.3
[N II] $\lambda 6548$	90 \pm 40	131 \pm 13	...	1400 \pm 300	0.72 \pm 0.11	34.6 \pm 3.6	...	37.2 \pm 4.1	...
H α $\lambda 6563$	496 \pm 97	1150 \pm 110	2.35 \pm 0.26	19000 \pm 2000	28.4 \pm 2.8	272 \pm 27	33.1 \pm 3.4	230 \pm 23	119 \pm 13
[N II] $\lambda 6584$	280 \pm 64	407 \pm 41	1.02 \pm 0.14	4370 \pm 550	2.41 \pm 0.26	92.3 \pm 9.3	2.73 \pm 0.51	86.2 \pm 8.8	20.0 \pm 3.2
[S II] $\lambda 6717$	114 \pm 28	149 \pm 16	...	4250 \pm 490	4.40 \pm 0.45	65.6 \pm 6.8	...	59.8 \pm 6.8	27.4 \pm 3.7
[S II] $\lambda 6731$	62 \pm 19	111 \pm 11	...	3210 \pm 390	2.77 \pm 0.29	48.4 \pm 5.1	...	35.9 \pm 4.6	23.6 \pm 3.4

Notes.

Rest emission-line fluxes in units of 10^{-17} erg s $^{-1}$ cm $^{-2}$ before extinction correction. Errors include statistical measurement uncertainties. Column headings designate the SN names whose host-galaxy line fluxes are presented; see Table 2 for the corresponding galaxy names. We do not list fluxes of the hosts of SN 2002ap, 2005da, and 2005fk, since no emission lines were detected in the galaxy spectra.

^a Central spectra also represent spectra taken at the SN position since the SN occurred in the galaxy nucleus. See Table 2.

Table 5
Galaxy Emission-Line Measurements at SN Position if Different from Galaxy Center

Emission line	SN 1997ef	SN 1998ey	SN 2003jd	SN 2005kz	SN 2005nb
[O II] $\lambda\lambda 3726, 29$	960 \pm 100	...	717 \pm 75	334 \pm 35	1170 \pm 130
[Ne III] $\lambda 3869$	19.4 \pm 2.8
He I+H ζ $\lambda 3889$	27.1 \pm 3.4
H ϵ $\lambda 3970$	30.0 \pm 3.7
H δ $\lambda 4101$	117 \pm 41	...	57.2 \pm 6.2
H γ $\lambda 4340$	188 \pm 27	...	99.0 \pm 10.2	...	174 \pm 40
H β $\lambda 4861$	478 \pm 51	73 \pm 12	229 \pm 24	656 \pm 12	376 \pm 45
[O III] $\lambda 4959$	55 \pm 16	...	116 \pm 14	...	153 \pm 28
[O III] $\lambda 5007$	223 \pm 30	...	342 \pm 36	115 \pm 17	455 \pm 52
[O I] $\lambda 6300$	13.1 \pm 4.9	158 \pm 18	...
[N II] $\lambda 6548$	161 \pm 23	22.8 \pm 7.1	23.6 \pm 4.7	...	85 \pm 13
H α $\lambda 6563$	1730 \pm 170	277 \pm 29	752 \pm 76	1660 \pm 170	1510 \pm 150
[N II] $\lambda 6584$	581 \pm 62	133 \pm 16	98 \pm 11	1300 \pm 130	299 \pm 33
[S II] $\lambda 6717$	308 \pm 36	...	110 \pm 11	...	131 \pm 16
[S II] $\lambda 6731$	226 \pm 28	...	83.6 \pm 8.9	...	125 \pm 16

Notes.

Rest emission-line fluxes in units of 10^{-17} erg s $^{-1}$ cm $^{-2}$ before extinction correction. Errors include statistical measurement uncertainties. Column headings designate the SN names whose host-galaxy line fluxes are presented; see Table 2 for the corresponding galaxy names.

4. DERIVED HOST-GALAXY PROPERTIES

4.1. Galaxy Luminosities

We drew the host-galaxy luminosities from the Lyon-Meudon Extragalactic Database (HyperLEDA)¹⁸ as their sample has been homogeneously compiled. We adopted as galaxy luminosities the values listed as *mabs* in HyperLEDA, i.e. the absolute *B*-band magnitude, M_B , corrected for Galactic and internal extinction and k-corrections.

We applied a similar procedure to derive absolute magnitudes for the hosts of Sloan SN that were not listed in HyperLEDA. We retrieved the host-galaxy Petrosian magnitudes from SDSS DR5¹⁹ and corrected for Galactic extinction using the tabulated reddening values and a standard Galactic reddening law with $R_V = 3.1$ (Cardelli et al. 1989). We applied k-corrections

calculated via *kcorrect* (v.3.2²⁰), which was developed by Blanton et al. (2003) for use with the SDSS filter set, in order to obtain the absolute *B*-band magnitude M_B . The full list is given in Column 2 of Tables 6 and 7.

4.2. Metallicities and Star-Formation Rates

The nebular oxygen abundance is the canonical choice of metallicity indicator for ISM studies, since oxygen is the most abundant metal in the gas phase, only weakly depleted, and exhibits very strong nebular lines in the optical wavelength range (Tremonti et al. 2004; Kobulnicky & Kewley 2004). Thus, well-established diagnostic techniques have been developed (e.g., Osterbrock 1989; Pagel et al. 1979). We compute host gas-phase oxygen abundance for both SN Ic (broad) and SN Ic (broad & GRB) using three different and independent metallicity diagnostics. Using three independent calibrations that utilize

¹⁸ See <http://leda.univ-lyon1.fr/>.

¹⁹ See <http://cas.sdss.org/dr5/en/tools/explore/>.

²⁰ See <http://cosmo.nyu.edu/blanton/kcorrect/>.

Table 6
Derived Central Properties of Host Galaxies of SN Ic (broad)

SN	M_B (mag)	$\log(\text{O}/\text{H}) + 12$ KD02 ^a	$\log(\text{O}/\text{H}) + 12$ M91 ^a	$\log(\text{O}/\text{H}) + 12$ PP04-O3N2 ^a	$L(\text{H}\alpha)^b$ ($10^{40} \text{ erg s}^{-1}$)	SFR^b ($M_\odot \text{ yr}^{-1}$)	$n_e(\text{S II})$ (cm^{-3})	$E(B - V)$ (mag)
SN 1997dq	-20.1	$9.15^{+0.36}_{-0.19}$ c	>0.11	>0.01	<10	...
SN 1997ef	-20.2	$8.93^{+0.01}_{-0.01}$...	$8.89^{+0.03}_{-0.03}$	1.2	0.09	90	0.48
SN 2002ap	-20.6	$9.10^{+0.04}_{-0.04}$	$9.04^{+0.05}_{-0.05}$	$8.82^{+0.05}_{-0.05}$
SN 2003bg	-17.5	$9.03^{+0.03}_{-0.03}$ c	> 10^{-4}	> 10^{-5}
SN 2003jd	-20.3	$8.80^{+0.02}_{-0.03}$...	$8.54^{+0.03}_{-0.03}$	36.3	2.9	110	0.32
SN 2005da	-21.4
SN 2005fk	-21.0
SN 2005kr ^d	-17.4	$8.63^{+0.03}_{-0.03}$	$8.64^{+0.01}_{-0.01}$	$8.24^{+0.01}_{-0.01}$	2.14	0.17	<10	0.10
SN 2005ks ^d	-19.2	$8.87^{+0.02}_{-0.03}$	$8.71^{+0.03}_{-0.04}$	$8.63^{+0.01}_{-0.01}$	14.0	1.11	80	0.26
SN 2005kz	-20.9
SN 2006nx ^d	-18.9	$8.53^{+0.10}_{-0.14}$	$8.48^{+0.09}_{-0.10}$	$8.24^{+0.04}_{-0.03}$	5.48	0.43	...	0.40
SN 2006qk ^d	-17.9	$8.82^{+0.04}_{-0.05}$	$8.61^{+0.07}_{-0.08}$	$8.75^{+0.02}_{-0.03}$	7.88	0.62	<10	0.52
SN 2007l ^d	-16.9	$8.71^{+0.03}_{-0.04}$ c	...	$8.39^{+0.40}_{-0.17}$	0.30	0.02	290	0.34

Notes.

^a Extinction-corrected oxygen abundances derived using the calibrations of Kewley & Dopita (2002, KD02), McGaugh (1991, M91), and Pettini & Pagel (2004), using the [O III]/[N II] calibration (PP04-O3N2). See Section 4.2 for details.

^b Extinction-corrected values. Lower limits are indicated if they could not be extinction corrected (when H β could not be observed).

^c Oxygen abundance computed using the N II/H α method.

^d Central spectra also represent spectra taken at the SN position since the SN occurred in the galaxy center. See Table 2.

Table 7
Derived Properties of Host Galaxies of SN Ic (broad) at SN Position if Different from Galaxy Center

SN	M_B (mag)	$\log(\text{O}/\text{H}) + 12$ KD02 ^a	$\log(\text{O}/\text{H}) + 12$ M91 ^a	$\log(\text{O}/\text{H}) + 12$ PP04-O3N2 ^a	$L(\text{H}\alpha)^b$ ($10^{40} \text{ erg s}^{-1}$)	SFR^b ($M_\odot \text{ yr}^{-1}$)	$n_e(\text{S II})$ (cm^{-3})	$E(B - V)$ (mag)
SN 1997dq	-20.1	$8.95^{+0.37}_{-0.21}$ c
SN 1997ef	-20.2	$8.93^{+0.04}_{-0.04}$	$8.84^{+0.02}_{-0.03}$	$8.69^{+0.02}_{-0.03}$	0.92	0.07	70	0.24
SN 1998ey	-21.8	$9.08^{+0.04}_{-0.04}$	0.31	0.02	...	0.12
SN 2002ap	-20.6	$8.62^{+0.06}_{-0.06}$ d	$8.56^{+0.07}_{-0.07}$ d	$8.38^{+0.06}_{-0.06}$ d
SN 2003bg	-17.5	$8.83^{+0.10}_{-0.10}$ c
SN 2003jd	-20.3	$8.59^{+0.05}_{-0.05}$	$8.62^{+0.02}_{-0.02}$	$8.39^{+0.02}_{-0.02}$	0.83	0.07	120	0.14
SN 2005nb	-21.3	$8.65^{+0.08}_{-0.09}$	$8.56^{+0.03}_{-0.03}$	$8.49^{+0.03}_{-0.03}$	4.33	0.34	480	0.34

Notes.

^a Extinction-corrected oxygen abundances derived using the calibrations of Kewley & Dopita (2002, KD02), McGaugh (1991, M91), and Pettini & Pagel (2004), using the [O III]/[N II] calibration (PP04-O3N2). See Section 4.2 for details.

^b Extinction-corrected values. Lower limits are indicated if they could not be extinction corrected (when H β could not be observed).

^c Extrapolated using central oxygen abundances from Table 6 and assuming standard metallicity gradient. See the text for details.

^d Extrapolated using central oxygen abundances from Table 6 and measured M 74 metallicity gradient. See the text for details.

different sets of lines for computing the oxygen abundance, we can check if any of our results depend on the choice of diagnostic. Furthermore, since different metallicity calibrations can have large systematic offsets between each other (Ellison et al. 2005; Ellison & Kewley 2005; Kewley et al. 2007), we compute abundances for host galaxies of both SN Ic (broad) and SN Ic (broad & GRB) in the same scale and compare their relative values. The three well-known diagnostics used here are: (1) the iterative strong-line diagnostics calibrated by Kewley & Dopita (2002) (henceforth KD02) and updated by Kobulnicky & Kewley (2004), (2) the calibration by McGaugh (1991) (henceforth M91), and (3) the diagnostic of Pettini & Pagel (2004) in the direct electron temperature (T_e) scale. Details about each calibration technique will be given below. For the SN Ic (broad), we furthermore list central abundances in Table 6 and those at the SN position separately (Table 7) as spiral galaxies possess observed radial metallicity gradients, from metal-rich centers to metal-poor outskirts (e.g., van Zee et al. 1998; Bell & de Jong 2000; Kewley et al. 2005). For the SN observed with GRBs, we consulted the literature for

the emission-line fluxes at the GRB-SN sites (Table 1) and list the abundances computed with the same three diagnostics in Table 8.

KD02 use a host of stellar population synthesis and photoionization models to derive their metallicity diagnostics. Oxygen abundances derived iteratively in this manner are listed in Column 3 of Tables 6–8, corrected for extinction (Column 9). For the metallicity range of $\log(\text{O}/\text{H}) + 12 \geq 8.5$, the KD02 method mainly uses the [N II] $\lambda 6584$ /[O II] $\lambda 3727$ ratio, while for the low-metallicity regime, the R_{23} diagnostic, defined as $R_{23} = ([\text{O II}] \lambda 3727 + [\text{O III}] \lambda \lambda 4959, 5007)/\text{H}\beta$, is usually employed. If neither H β nor [O II] $\lambda 3727$ are observed, we adopt the [N II] $\lambda 6584/\text{H}\alpha$ method from Kobulnicky & Kewley (2004) with the KD02 calibration, assume a normal ionization parameter ($q = 2 \times 10^7 \text{ cm s}^{-1}$) and note those cases in the tables.

As alternatives, we also provide metallicity determinations using the well-known strong-line calibration of McGaugh (1991) (henceforth M91) in Column 4 and Pettini & Pagel (2004) (henceforth PP04) in Column 5. M91 provides a

Table 8
Derived Properties of Host Galaxies of SN Ic (broad & GRB) at GRB Position

GRB/SN name	M_B (mag)	$\log(\text{O}/\text{H}) + 12$ KD02 ^a	$\log(\text{O}/\text{H}) + 12$ M91 ^a	$\log(\text{O}/\text{H}) + 12$ T_e ^a	$L(\text{H}\alpha)^b$ ($10^{40} \text{erg s}^{-1}$)	SFR ^b ($M_\odot \text{yr}^{-1}$)	$n_e(\text{S II})$ (cm^{-3})
GRB 980425/SN 1998bw	-17.6	8.5	8.3	...	4.14	0.19	...
GRB 031203/SN 2003lw	-21.0	8.1	8.0	7.8 ^c	217.0	9.20	300
020903	-18.8	8.3	8.3	8.0 ^c	3.76	0.16	...
GRB/XRF 060218/SN 2006aj	-15.9	8.1	8.0	7.5 ^c	0.82	0.03	...
GRB 030329/SN 2003dh	-16.5	8.0	7.9	7.5 ^d	3.00	0.13	...

Notes.

^a Extinction-corrected oxygen abundances derived using the calibrations of Kewley & Dopita (2002, KD02), McGaugh (1991, M91), and in the T_e scale. See Section 4.2 for details.

^b Extinction-corrected values.

^c From T_e method and measured [O III] $\lambda 4363$.

^d From the KD02- T_e conversion using Equation (3) in Kewley et al. (2007).

theoretical calibration of the R_{23} parameter via photoionization models that produce oxygen abundances that are comparable in accuracy to direct methods that rely on the measurement of nebular temperature. The PP04 calibration, on the other hand, is predominantly based on an empirical fit to the electron temperature (T_e)-abundances (using the lines of [O III] $\lambda 4363$ and [O II] $\lambda 3727$) of H II regions. This method is often referred to as the “direct” abundance method, as accurate abundance measurements can be obtained directly from line ratios of auroral to nebular line intensities, such as [O III] $\lambda 4363/\lambda 5007$ that indicate the electron temperature. However, the T_e method saturates at higher metallicities ($\log(\text{O}/\text{H}) + 12 \geq 8.4$), probably due to the additional cooling of [O III] lines in the IR which is not accounted for in the current T_e prescription, and hence PPO4 include six R_{23} -derived metallicities to extrapolate to higher metallicities. The PPO4 scale is typically ~ 0.2 dex lower than the theoretical strong-line methods such as KD02. The exact cause of this discrepancy is highly debated (for a discussion see e.g., Garnett et al. 2004a; Garnett et al. 2004b; Stasińska 2005), and it might be due to temperature variations that are not considered properly in the T_e prescription (Bresolin 2006). For the host galaxies of SN Ic (broad), we used the recommended [O III]/[N II]-based prescription of PP04 (henceforth called PP04-O3N2). For the host galaxies of SN Ic (broad & GRB), we list in Table 8 their oxygen abundances in the T_e scale, either via direct measurements of [O III] $\lambda 4363$ or by converting KD02 abundances into T_e -based ones. Since the PP04 calibration is tied to the T_e -abundances, the inter comparison should be valid. We note that the GRB–SN abundances in the scales of KD02 and T_e were already computed in Kewley et al. (2007). We furthermore use the direct T_e -based abundance for the host of GRB/XRF 060218/SN 2006aj as derived from the recent detection of [O III] $\lambda 4363$ (Wiersema et al. 2007), which is the same as the T_e -converted KD02 abundance from Kewley et al. (2007).

We compute the uncertainties in the measured metallicities by explicitly including the statistical uncertainties of the line flux measurements and those in the derived SN host-galaxy reddening, and by properly propagating them into the metallicity determination. Details are discussed in Section 4.3.

For M 74, the host of SN 2002ap, we took the measured emission-line fluxes of individual H II regions in M 74 and their de-projected galactocentric radii from McCall et al. (1985); Ferguson et al. (1998); van Zee et al. (1998); Bresolin et al. (1999); and Castellanos et al. (2002). Having computed the oxygen abundances in the three metallicity scales, we fit for the observed M 74 abundance gradient and obtain radial gradients of $-0.49 \pm 0.04 \text{ dex}/\rho_{25}$, $-0.49 \pm 0.05 \text{ dex}/\rho_{25}$, and $-0.45 \pm$

$0.05 \text{ dex}/\rho_{25}$, in the scales of the KD02, M91 and PP04(O3N2), respectively, where ρ_{25} stands for the isophotal radius. With an extrapolated central metallicity as listed in Table 6 and the appropriate gradient, we compute the metallicity at the radial de-projected distance of SN 2002ap ($4'38''$) and list them in Table 7. We note that the oxygen abundance at the SN position is similar to the value quoted in Smartt et al. (2002) and Crockett et al. (2007) in the appropriate scales. The uncertainty in the value of ρ_{25} for M 74 introduces the (small) uncertainty of 0.02 dex in the oxygen abundance value, which we include in the uncertainty budget.

For NGC 3810 and MCG-05-10-15, the hosts of SN 1997dq and 2003bg, we do not possess spectra taken at the SN positions, which are $52''$ and $30''$, respectively, from the galaxy centers. At the distance of SN 1997dq (~ 18 Mpc, from HyperLEDA) and of SN 2003bg (~ 16 Mpc, from HyperLEDA), the SN de-projected galactocentric distances amount to ~ 4.5 kpc and 2.4 kpc, respectively. Assuming usual metallicity gradients of $\sim -0.05 \text{ dex kpc}^{-1}$ for $M_B = -20$ mag spirals and of $\sim -0.1 \text{ dex kpc}^{-1}$ for $M_B = -17.5$ mag galaxies (Garnett et al. 1997; Henry & Worthey 1999), i.e., similar to the host galaxies, we adopt SN metallicity values that are 0.2 dex lower than that of the nucleus for both galaxies (see Table 7). In order to account for the uncertainty in the extrapolated abundances at the SN site, we added in quadrature the spread in metallicity gradients (choosing a conservative value of 0.1 dex) observed for galaxies of corresponding luminosity to the uncertainty in the central abundance.

We note that we were not able to compute reliable metallicities and star-formation rates (SFRs) for the host galaxy of SN 2005kz. Its spectrum is dominated by an active galactic nucleus (AGN) and its line ratios of [N II]/H α , [O III]/H β , and [O I]/H α are characteristic of a composite starburst/Seyfert2 object (Kewley et al. 2006). Thus, we only list SN 2005kz’s host galaxy M_B in Table 6, along with the M_B of hosts of SN 2005da and 2005fk.

Using the H α emission-line strengths listed in Tables 4 and 5, we derive extinction-corrected local H α luminosities and extinction-corrected local SFRs (Kennicutt 1998), and list them in Columns 6 and 7 of Tables 6–8. We note that these values are lower limits to the global SFR since the galaxies have larger angular diameters than the slit sizes used, except for SDSS J030829.66–005320.1, the host galaxy of SN 2005kr. When available, we use the line ratio of S II $\lambda 6717$ and S II $\lambda 6731$ combined with the Mappings photoionization code (Sutherland & Dopita 1993) and a five-level model to compute electron densities in the S+ zone (Column 8).

4.3. Uncertainties in Metallicity Measurements

We explicitly include the effect of the statistical errors in the line measurements on the metallicity determinations. For each metallicity diagnostic, we compute the minimum and maximum oxygen abundance values for the given statistical uncertainties in the line measurements and assign them as bounds for the most positive and negative errors. These are listed in Tables 6 and 7, directly following the reported abundance value as determined from the measured line values. In the computation, we also include the effect of the statistical error in the $H\alpha/H\beta$ ratio that influences the measured Balmer decrement and therefore the derived reddening. Because of logarithmic dependence of the metallicity diagnostics on line ratios, the computed abundance uncertainties are sometimes not symmetric around the reported values. Furthermore, we checked whether a change in the case B recombination value from 2.85 to, e.g., 3.1 (typical of AGNs) makes a difference in the derived metallicities from $[N II]/[O II]$, and the effect is minor (<0.03 dex).

In the optical, the choice of extinction curve makes negligible difference to the extinction correction of optical line ratios (see e.g., the review by Calzetti 2001). We have tested this ourselves by applying three different extinction curves to $[N II]/[O II]$: the Whitford Reddening curve, as parameterized by Miller & Mathews (1972), the parameterization by Cardelli et al. (1989), and that by Osterbrock (1989). We find that metallicities derived from $[N II]/[O II]$ using different optical extinction curves are identical. The same conclusion was obtained by Moustakas & Kennicutt (2006a, 2006b), who explored the effect of different extinction curve on oxygen abundance determinations of a sample of 417 nearby galaxies with a diverse range of galaxy types and histories.

For the SN–GRB sample, the line flux errors are not available for the majority of GRB host spectra in the literature and we therefore assign a uniform conservative error of 0.1 dex.

5. DISCUSSION

We find that the host galaxies of broad-lined SN Ic have the following properties: they are mid- to late-type spirals (consistent with the host-galaxy morphological classifications found for the host galaxies of SN Ib and SN Ic in van den Bergh et al. 2005 and references therein), their B -band luminosities range between $-17 < M_B < -22$ mag, and their central oxygen abundances span $8.63 < 12 + \log(O/H)_{KD02} < 9.15$. Along with their SFRs and electron densities, they appear to conform to the general population of normal local star-forming galaxies (for comparison with SDSS star-forming galaxies, see Section 5.1 and Figure 5).

5.1. Comparison with the SN–GRB Sample

It is the main goal of this study to compare the physical characteristics of host galaxies of SN Ic (broad) that had no observed GRBs to those of SN–GRB hosts.

First, we find that the SFR values are similar between the two samples, with $SFR(H\alpha) \sim 0.1\text{--}3 M_{\odot} \text{ yr}^{-1}$. One exception appears to be MCG-05-10-15, the host of SN 2003bg, which has a value of $10^{-5} M_{\odot} \text{ yr}^{-1}$, not corrected for extinction. However, most of our local SFR values of SN Ic (broad) are lower limits to the global values, and thus they are probably larger than those of the GRB–SN host sample. Furthermore, considering the much smaller masses for the GRB hosts as indicated by their lower luminosities, the *specific* SFRs (SFRs normalized to galaxy mass) of GRB hosts are larger than those of SN Ic hosts, and of

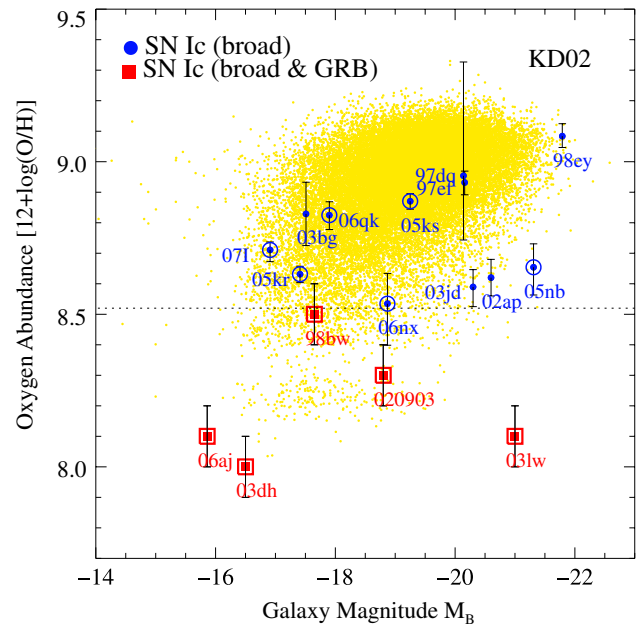


Figure 5. Host-galaxy luminosity (M_B) and host-galaxy metallicity (in terms of oxygen abundance) at the sites of nearby broad-lined SN Ic (“SN Ic (broad)”: blue filled circles) and broad-lined SN Ic connected with GRBs (“SN (broad & GRB)”: red filled squares; see also Stanek et al. 2006; Kewley et al. 2007). Extra circles and squares designate SN which were found in a non-targeted fashion. The oxygen abundances are in the Kewley & Dopita (2002) (KD02) scale and represent the abundance at the SN position. Due to radial metallicity gradients, the gas abundance at the SN position is lower than the central galaxy abundance for some SN (compare Tables 6 and 7). Labels represent the SN names while one (“020903”) refers to its associated GRB. Yellow points are values for local star-forming galaxies in SDSS (Tremonti et al. 2004), re-calculated in the Kewley & Dopita (2002) scale for consistency, and illustrate the empirical luminosity–metallicity (L – Z) relationship for galaxies. Host environments of GRBs are more metal poor than host environments of broad-lined SN Ic where no GRB was observed, for a similar range of host-galaxy luminosities. The dotted line at $12 + \log(O/H)_{KD02} \sim 8.5$ designates the apparent dividing line between SN with and without observed GRBs.

(A color version of this figure is available in the online journal)

SDSS galaxies in general (Christensen et al. 2004; Gorosabel et al. 2005; Sollerman et al. 2005; Savaglio et al. 2006; Thoene et al. 2007). A comparison between the electron densities does not yield any statistical significant results, as only one SN–GRB host has a measured electron density. All measured electron densities lie within the range of observed values for galaxies and H II regions.

Next, Figure 5 shows the main result of our comparison: we plot host-galaxy metallicity (as expressed in terms of oxygen abundance $12 + \log(O/H)$ with the KD02 calibration) and host-galaxy luminosity (M_B) of broad-lined SN Ic without observed GRBs (called “SN Ic (broad),” circles) and with GRBs (called “SN Ic (broad & GRB),” squares). Objects whose host galaxies had not been targeted during the discovery have an extra circle (for SN without GRBs) or an extra square (for SN with GRBs) around their plotted symbol. We note that three of the five broad-lined SN Ic found in the lower luminosity galaxies ($M_B > -19$ mag) were discovered by the SDSS-II SN Survey, which is a galaxy-impartial survey. For the broad-lined SN Ic we only plot abundances measured at or extrapolated to the SN position. These plotted values are sometimes lower than the values we measure for the center of the same host galaxies (see Table 6) presumably due to metallicity gradients as discussed in Section 4.2. The SN–GRB host abundances also reflect the

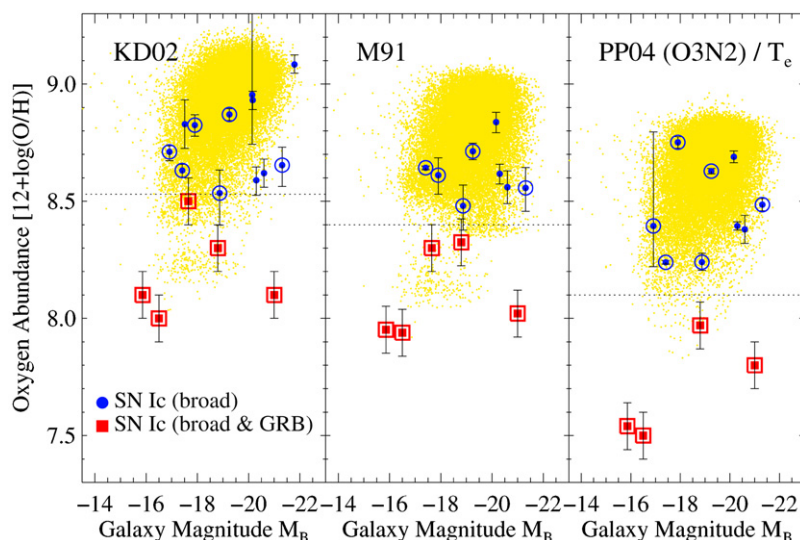


Figure 6. Similar to Figure 5, but using different metallicity diagnostics; Kewley & Dopita (2002) (KD02) as in Figure 5 (left); McGaugh (1991) (M91, middle); and Pettini & Pagel (2004) (PP04-O3N2), which is effectively on the T_e scale, (right). As before, host-galaxy luminosity (M_B) and host-galaxy metallicity (in terms of oxygen abundance) at the SN site are plotted for nearby broad-lined SN Ic (“SN Ic (broad)”; blue filled circles) and for broad-lined SN Ic connected with GRBs (“SN (broad & GRB)”; red filled squares). Extra circles and squares designate SN which were found in a non-targeted fashion. Host environments of GRBs are more metal poor than environments of broad-lined SN Ic where no GRB was observed, independent of the abundance scale used. Yellow dots designate the SDSS galaxy values calculated in the respective metallicity scales.

(A color version of this figure is available in the online journal)

metallicity at the SN–GRB position, since they were either measured specifically at the SN position (for GRB 980425/SN 1998bw) or the SN reside in the nucleus of their dwarf-galaxy hosts that are chemically homogeneous (Kobulnicky & Skillman 1997). Due to the short lifetimes of the massive SN progenitor stars ($t \lesssim 10$ million years for $M_{ZAMS} \gtrsim 20 M_{\odot}$, e.g., Woosley et al. 2002), we regard the metallicities at the SN position as natal metallicities.

For reference, we also plot the luminosities of local ($0.005 < z < 0.2$) SDSS star-forming galaxies from Tremonti et al. (2004). The plotted oxygen abundances were re-calculated in the KD02 scale, using the published emission-line fluxes, to be internally consistent. We used the DR2 values with a supernova remnant (SNR)-cut of 5 for the emission-line fluxes. Their loci on Figure 5 illustrate the well-studied luminosity–metallicity (L – Z) relationship for disk galaxies (e.g., Rubin et al. 1984; Garnett 2002; Tremonti et al. 2004), which has been also observed for dwarf irregular galaxies (Searle & Sargent 1972; Lequeux et al. 1979; Skillman et al. 1989; Pilyugin 2001; Garnett 2002) and for blue compact galaxies (Campos-Aguilar et al. 1993; Shi et al. 2005). We note that the SDSS metallicities were derived using fibers $3''$ in diameter, corresponding to a mean projected fiber size of ~ 4.6 kpc for that sample (Tremonti et al. 2004), and that they therefore generally reflect central metallicities (see also Kewley et al. 2005). Hence, a detailed comparison between the distribution of abundances at the SN sites and those of SDSS galaxies is not warranted, and the SDSS loci should be regarded as indicating a general trend.

There is a bimodal distribution of host-galaxy luminosities and metallicities: the luminosities of the hosts for the SN–GRBs are generally low, while the SN Ic (broad) hosts extend to high galaxy luminosities. What is more, the SN–GRBs have low metallicity environments while SN Ic (broad) are found in systematically higher metallicity environments. We plot as a dotted line the value of $12 + \log(O/H)_{KD02} \sim 8.5$ that appears to be the dividing line for the oxygen abundance between SN

with and without observed GRBs. While this GRB host-galaxy preference compared to other galaxies has been noted before (e.g., Prochaska et al. 2004; Gorosabel et al. 2005; Sollerman et al. 2005; Modjaz et al. 2006; Stanek et al. 2006; Kewley et al. 2007), we emphasize that we are comparing now the host galaxies of SN with the same spectral characteristics. Thus, our comparison includes any conditions required to produce envelope-stripped core-collapse SN and we can test whether low metal abundance is a sufficient condition for the evolution of the massive progenitor through the stages that lead to a GRB jet. Using the host metallicities with the KD02 calibration of SN Ic (broad & GRB) and of SN Ic (broad) found in non-targeted fashion, we conduct a simple Kolmogorov–Smirnov (K–S) test. We find that the probability that both sets of host metallicities have been drawn from the same parent population is low, namely $\sim 3\%$.

Moreover, we plot in Figure 6 the comparison between the two host samples and the local SDSS galaxies in the metallicity scales of M91 and PP04-O3N2, with the latter being effectively in the T_e scale. While the absolute values of the abundances are different in different scales, as expected, the bimodal distribution persists in each scale, and thus is independent of the choice of metallicity diagnostic. The K–S test applied to the host abundances of SN Ic (broad & GRB) and SN Ic (broad) found in a non-targeted fashion yields low probabilities of 4% (M91-based abundances) and 3% (T_e -based abundances) that they are drawn from the same population. For each scale, we plot as a dotted line the boundary that separates the two samples: $12 + \log(O/H)_{M91} \sim 8.4$ and $12 + \log(O/H)_{T_e} \sim 8.1$. Although our sample is small our findings are consistent with the hypothesis that low metal abundance is the cause of some very massive stars becoming SN–GRBs.

Of course, a question of interest for GRB modelers is how these cutoff values in oxygen abundance compare to solar metallicity. The answer is not clear due to the problems that plague absolute metallicity determination: it depends on which

of the three metallicity scales is adopted and whether one uses the high value for solar oxygen abundance ($12 + \log(\text{O}/\text{H}) = 8.9$, Delahaye & Pinsonneault 2006) or the lower, revised solar abundance ($12 + \log(\text{O}/\text{H}) = 8.7$, Asplund et al. 2005). Thus, the cutoff value can range between 0.2 and 0.6 Z_{\odot} . Nevertheless, our main conclusions do not depend on the absolute metallicity scale.

We note that Tremonti et al. (2004) computed the metallicity of the host galaxy of SN 2007I with their diagnostics, using the same SDSS emission-line spectrum we used. Their value, $12 + \log(\text{O}/\text{H})_{\text{Tremonti04}} = 8.3$, is 0.4 dex lower than $12 + \log(\text{O}/\text{H})_{\text{KD02}} = 8.71 \pm 0.04$, but similar to $12 + \log(\text{O}/\text{H})_{\text{PP0403N2}} = 8.39^{+0.4}_{-0.17}$. We attribute this difference to the absence of [O II] in the galaxy spectrum which precludes the usage of the reliable KD02 methods (using [N II]/[O II] or R_{23}), and instead necessitates using [N II]/ $H\alpha$. Thus, the reliable metallicity for this galaxy is in the PP04 scale. Nevertheless, this caveat does not change our conclusions as the GRB–SN metallicities are even lower than $12 + \log(\text{O}/\text{H})_{\text{PP0403N2}} = 8.4$.

At face value, our results differ from various studies in the literature, which have concluded that high- z GRB hosts are not necessarily low-metallicity systems. However, there might be intrinsic differences in GRB population at low and high z —as mentioned, the low- z GRBs might constitute a different class of low-luminosity GRBs that are not detected at higher z (Cobb et al. 2006; Liang et al. 2007; Guetta & Della Valle 2007). Moreover, most of the techniques for measuring abundances at higher z are different from our direct approach: they either use absorption techniques in GRB afterglows (Prochaska et al. 2007 and references therein) or infer the metallicity using galaxy luminosity and color via the L – Z relation (Berger et al. 2006). Attempts to directly measure GRB host metallicities at higher redshifts via emission-line diagnostics remain inconclusive (Savaglio et al. 2006, S. Savaglio 2008, in preparation).

Recently, Wolf & Podsiadlowski (2007) suggested that if there were a sharp cutoff for the metallicity dependence of cosmological GRBs, assuming that the GRB hosts follow the standard L – Z relationship at $z \sim 0.7$, it would lie at around $12 + \log(\text{O}/\text{H})_{\text{lim}} \sim 8.7 \pm 0.3$ in the scale of Kobulnicky & Kewley (2004). They claimed to rule out GRB models that require sharp metallicity cutoffs well below one-half the solar abundance (assuming the value of 8.7 as the solar oxygen abundance), since those models would predict GRB hosts that need to be much less luminous than the observed hosts in the sample of Fruchter et al. (2006). Interestingly, even though their assumptions rely on the conforming behavior of GRB hosts, and they investigate cosmological GRBs, their findings are consistent with our results. Ongoing attempts to directly measure host-galaxy metallicities of cosmological GRBs (e.g., Savaglio et al. 2006) are expected to clarify this debate, though long integration times and NIR spectra will be required for the bulk of the cosmological GRBs due to their high redshift (with a mean $z \sim 3$ for the *Swift* GRBs).

5.2. Viewing Angle Effects and Caveats

Cosmological GRBs are highly collimated events, with beaming angles $\theta \sim 4$ –10 deg (Frail et al. 2001; Guetta et al. 2005), while the low-luminosity, nearby GRBs appear to be less beamed (Guetta & Della Valle 2007). Thus, one might argue that the lack of observed gamma-ray emission for the SN Ic (broad) presented in this study is due to viewing angle effects, i.e. the GRB occurred but our line-of-sight was not aligned with the jet axis.

We have good reason to believe that this is probably not the case for at least six of the 12 objects in our sample. Soderberg et al. (2006b) searched for radio emission in 68 local SN Ib and SN Ic at late times (after 0.5–20 years), when the GRB, if present, is expected to become isotropic and emit in the radio regime. They did not detect late-time radio emission and therefore exclude an off-axis jet-driven SN engine in the following SN of our sample: SN 1997dq, SN 1997ef, SN 1998ey, SN 2002ap, SN 2003jd, and, in addition SN 2005da (Soderberg & Kulkarni 2005) and SN 2005kz (Soderberg 2005). We note that the conclusions of Soderberg et al. (2006b) rely on modeling GRB radio properties based on those observed for GRB 980425/SN 1998bw. Including GRB/XRF 060218/SN 2006aj, Soderberg et al. (2006c) infer that less than one in three broad-lined SN may have a radio luminosity comparable to GRB/XRF 060218/SN 2006aj. For SN 2003bg, strong early-time X-ray and radio emission was detected (Soderberg et al. 2003; Pooley & Lewin 2003) and interpreted as signs of interactions between SN ejecta and dense circumstellar matter (CSM) (Soderberg et al. 2006a).

There was no such radio search for emission in the SN found by the Sloan-II SN survey from our sample. Thus, the viewing angle issue remains a caveat for these SN.

As noted above, Mazzali et al. (2005) argue for an off-axis jet in SN 2003jd, since they interpret double-peaked oxygen and magnesium profiles observed in its late-time spectra as signs of an aspherical, axisymmetric explosion caused by a jet. However, asphericities have been observed in other core-collapse SN (e.g., Leibundgut et al. 1991), most notably in SN 1987A (e.g., Wang et al. 2002), and might not necessarily signal the presence of a relativistic jet of material. Polarization studies suggest clear asphericity in ejecta of all types of core-collapse SN, which increases with decreasing envelope mass (see Leonard & Filippenko 2005 for a review). These results indicate that asphericity might be a ubiquitous feature of the conventional neutrino-driven process of core collapse, occasionally damped by the additional envelopes of hydrogen and helium. In order to fully observationally probe the range of geometries realized during the explosion of massive stars, a systematic study of late-time spectral features for a large sample of stripped-envelope core-collapse SN (i.e., SN Ib, Ic, Iib) is necessary. Such a study is presently underway and includes a SN Ib, SN 2004ao that displays a double-peaked profile of oxygen with the same width and characteristics as seen in SN 2003jd (Modjaz 2007; Modjaz et al. 2008).

Furthermore, Li (2006) describes tentative evidence for a relationship between E_{pk} , the peak of the gamma-ray spectrum of four GRBs with associated SN, and the peak luminosity (M_{SN}) of their associated SN, such that GRBs with harder gamma-ray spectra have associated SN that are more luminous. Furthermore, he suggests that the E_{pk} of the putative GRBs if they occurred in association with SN 2002ap and 1997ef would have been located in the UV regime due to the low SN luminosities and that those GRBs would have had very low gamma-ray energies (Li 2006). If true, those explosions would hardly qualify as bona fide “gamma-ray” bursts. In any case, caution should be exercised when extending a relationship based on four objects to a range outside that probed by the data, and future nearby GRBs–SN ought to be used to verify the E_{pk} – M_{SN} correlation of Li (2006).

Thus, we conclude that observations do not support associated off-axis GRBs with six broad-lined SN Ic, while we cannot exclude the possibility of off-axis GRBs in the SDSS–SN of our sample.

6. CONCLUSIONS AND SUMMARY

In this paper, we presented spectroscopic data of a statistically significant set of host galaxies of 12 nearby ($z < 0.14$) broad-lined SN Ic with no observed GRBs. Using the galaxy emission-line measurements corrected for stellar absorption and extinction, we derived central oxygen abundances and abundances at the SN position based on strong-line diagnostics that span $8.5 < 12 + \log(\text{O}/\text{H})_{\text{KD02}} < 9.1$ on the Kewley & Dopita (2002) scale, $8.5 < 12 + \log(\text{O}/\text{H})_{\text{M91}} < 8.9$ on the McGaugh (1991) scale, and $8.2 < 12 + \log(\text{O}/\text{H})_{\text{PP04}} < 8.9$ on the Pettini & Pagel (2004) scale, which effectively uses the T_e scale. Furthermore, we computed local SFRs for central regions, as well as for regions at the position of the SN, and drew from the literature the host-galaxy B -band luminosities, which range between $-17 < M_B < -22$ mag. This study, which constructed local chemical abundances for the locations of individual supernovae of Type Ic (broad), is the first of its kind. To our knowledge, a broader application of this approach to other core-collapse SN has not been carried out.

We compared the properties of our host sample with the properties of five nearby SN–GRB hosts, for which we derived chemical abundances using the same three metallicity diagnostics as for SN without observed GRBs. Broad-lined SN Ic without GRBs tend to consistently inhabit more metal-rich environments, and their host galaxies, for the *same* luminosity range ($-17 < M_B < -21$ mag), are systematically more metal rich than corresponding GRB host galaxies. The trend is independent of the choice of diagnostic and cannot be due to selection effects as we include six SN found in a similar non-targeted manner as GRBs–SN. The boundary between broad-lined SN Ic that have a GRB accompanying them and broad-lined SN Ic without a GRB lies at an oxygen abundance of $\sim 12 + \log(\text{O}/\text{H})_{\text{KD02}} \sim 8.5$, which corresponds to 0.2–0.6 Z_{\odot} depending on the adopted metallicity scale and solar abundance value. This correlation is consistent with the argument that (local) long-duration GRBs require low-metallicity environments for jet production. If this correlation holds up as the samples grow, it would be consistent with the idea that low metal abundance is a significant factor that allows a very massive star to become both a broad-lined SN Ic and a GRB when it collapses. On the other hand, if broad-lined SN Ic without off-axis GRBs are found in galaxies with low metal abundance, then a more complicated set of conditions than simply metal abundance will need to be considered.

Since 3/5 of the broad-lined SN Ic harbored in low-luminosity galaxies were found by the SDSS-II SN Survey, we note the importance of rolling, galaxy-impartial SN surveys to uncover the population of SN in dwarf galaxies. Future impartial, large and deep photometric surveys such as Pan-STARRS (Tonry & Pan-STARRS Team 2005), Skymapper (Granlund et al. 2006), and the Large Synoptic Survey Telescope (LSST) (Pinto 2004) will hence greatly contribute to the understanding and study of stellar explosions in different galactic environments. Finally, we recommend observational metallicity studies of a statistically significant set of SN Ib, SN Ic, broad-lined SN Ic, and SN II as to investigate any metallicity effects on the properties of core-collapse SN and on the extent of prior mass loss, which are expected on theoretical (e.g., Woosley et al. 2002; Woosley & Janka 2005) and stellar evolutionary grounds (Crowther & Hadfield 2006).

M.M. would like to thank Jesse Leaman for making data available before publication and John Moustakas for

compiling the published H II region line fluxes for M 74. We also acknowledge Christy Tremonti for making available the SDSS galaxy parameters in a convenient form. M.M. acknowledges helpful discussions with M. Geller, W. Brown, K. Rines, C. Tremonti, C. Stubbs, R. Narayan, N. Smith, and D. Sasselov. We thank the service observers of the 1.5 m FLWO for taking some of the spectra presented here.

Observations reported here were obtained at the MMT Observatory, a joint facility of the Smithsonian Institution and the University of Arizona, and at the F. L. Whipple Observatory, which is operated by the Smithsonian Astrophysical Observatory. Supernova research at Harvard University has been supported in part by the National Science Foundation grant AST06-06772 and R.P.K. in part by the Kavli Institute for Theoretical Physics NSF grant PHY99-07949. L.K. and J.E.G. are supported by a Hubble Fellowship.

Furthermore, this research has made use of NASA's Astrophysics Data System Bibliographic Services (ADS), the HyperLEDA database, and the NASA/IPAC Extragalactic Database (NED) which is operated by the Jet Propulsion Laboratory, California Institute of Technology, under contract with the National Aeronautics and Space Administration.

Funding for the SDSS and SDSS-II has been provided by the Alfred P. Sloan Foundation, the Participating Institutions, the National Science Foundation, the U.S. Department of Energy, the National Aeronautics and Space Administration, the Japanese Monbukagakusho, the Max Planck Society, and the Higher Education Funding Council for England.

The SDSS is managed by the Astrophysical Research Consortium for the Participating Institutions. The Participating Institutions are the American Museum of Natural History, Astrophysical Institute Potsdam, University of Basel, Cambridge University, Case Western Reserve University, University of Chicago, Drexel University, Fermilab, the Institute for Advanced Study, the Japan Participation Group, Johns Hopkins University, the Joint Institute for Nuclear Astrophysics, the Kavli Institute for Particle Astrophysics and Cosmology, the Korean Scientist Group, the Chinese Academy of Sciences (LAMOST), Los Alamos National Laboratory, the Max Planck Institute for Astronomy (MPIA), the Max Planck Institute for Astrophysics (MPA), New Mexico State University, Ohio State University, University of Pittsburgh, University of Portsmouth, Princeton University, the United States Naval Observatory, and the University of Washington.

REFERENCES

- Asplund, M., Grevesse, N., & Sauval, A. J. 2005, in *Astronomical Society of the Pacific Conference Series*, Vol. 336, *Cosmic Abundances as Records of Stellar Evolution and Nucleosynthesis*, ed. T. G. Barnes, III, & F. N. Bash, 25
- Barentine, J., et al. 2005a, *Central Bureau Electronic Telegrams*, ed. D. W. E. Green, 247, 1
- Barentine, J., et al. 2005b, *Central Bureau Electronic Telegrams*, ed. D. W. E. Green, 304, 1
- Bassett, B., et al. 2006a, *Central Bureau Electronic Telegrams*, ed. D. W. E. Green, 743, 1
- Bassett, B., et al. 2006b, *Central Bureau Electronic Telegrams*, ed. D. W. E. Green, 762, 1
- Bell, E. F., & de Jong, R. S. 2000, *MNRAS*, 312, 497
- Berger, E., Fox, D. B., Kulkarni, S. R., Frail, D. A., & Djorgovski, S. G. 2006, arXiv astro-ph/0609170
- Bersier, D., et al. 2006, *ApJ*, 643, 284
- Blanton, M. R., et al. 2003, *ApJ*, 594, 186
- Blondin, S., Modjaz, M., Kirshner, R., Challis, P., & Calkins, M. 2007, *Central Bureau Electronic Telegrams*, ed. D. W. E. Green, 808, 1

- Bresolin, F. 2006, in *The Metal-Rich Universe* (La Palma, 2006 June), ed. G. Israelian, & G. Meynet (Cambridge: Cambridge Univ. Press) in press (arXiv [astro-ph/0608410](https://arxiv.org/abs/astro-ph/0608410))
- Bresolin, F., Kennicutt, Jr., R. C., & Garnett, D. R. 1999, *ApJ*, **510**, 104
- Bromley, B. C., Press, W. H., Lin, H., & Kirshner, R. P. 1998, *ApJ*, **505**, 25
- Brown, W. R., Kewley, L., & Geller, M. J. 2008, *AJ*, **135**, 92
- Burket, J., Swift, B., Li, W., & Briggs, D. 2003, IAU Circ., 8232, 1
- Calzetti, D. 2001, *PASP*, **113**, 1449
- Calzetti, D., Kinney, A. L., & Storch-Bergmann, T. 1994, *ApJ*, **429**, 582
- Campana, S., et al. 2006, *Nature*, **442**, 1008
- Campos-Aguilar, A., Moles, M., & Masegosa, J. 1993, *AJ*, **106**, 1784
- Cardelli, J. A., Clayton, G. C., & Mathis, J. S. 1989, *ApJ*, **345**, 245
- Castellanos, M., Díaz, A. I., & Terlevich, E. 2002, *MNRAS*, **329**, 315
- Chassagne, R. 2003, IAU Circ., 8082, 1
- Christensen, L., Hjorth, J., & Gorosabel, J. 2004, *A&A*, **425**, 913
- Cobb, B. E., Baily, C. D., van Dokkum, P. G., & Natarajan, P. 2006, *ApJ*, **645**, L113
- Connolly, A. J., Szalay, A. S., Bershad, M. A., Kinney, A. L., & Calzetti, D. 1995, *AJ*, **110**, 1071
- Crockett, R. M., et al. 2007, *MNRAS*, **381**, 835
- Crowther, P. A., & Hadfield, L. J. 2006, *A&A*, **449**, 711
- Delahaye, F., & Pinsonneault, M. H. 2006, *ApJ*, **649**, 529
- Della Valle, M., et al. 2003, *A&A*, **406**, L33
- Ellison, S. L., & Kewley, L. J. 2005, arXiv [astro-ph/0508627](https://arxiv.org/abs/astro-ph/0508627)
- Ellison, S. L., Kewley, L. J., & Mallén-Ornelas, G. 2005, *MNRAS*, **357**, 354
- Fabricant, D., Cheimets, P., Caldwell, N., & Geary, J. 1998, *PASP*, **110**, 79
- Ferguson, A. M. N., Gallagher, J. S., & Wyse, R. F. G. 1998, *AJ*, **116**, 673
- Filippenko, A. V. 1982, *PASP*, **94**, 715
- Filippenko, A. V., & Chornock, R. 2003, IAU Circ., 8084, 4
- Filippenko, A. V., Foley, R. J., & Matheson, T. 2005, IAU Circ., 8639, 2
- Filippenko, A. V., Foley, R. T., & Swift, B. 2003, IAU Circ., 8234, 2
- Filippenko, A. V., Li, W. D., Treffers, R. R., & Modjaz, M. 2001, in ASP Conf. Ser. 246: IAU Colloq. 183: Small Telescope Astronomy on Global Scales, ed. B. Paczynski, W.-P. Chen, & C. Lemme (San Francisco, CA: ASP), 121
- Foley, R. J., et al. 2003, *PASP*, **115**, 1220
- Frail, D. A., et al. 2001, *ApJ*, **562**, L55
- Fruchter, A. S., et al. 1999, *ApJ*, **519**, L13
- Fruchter, A. S., et al. 2006, *Nature*, **441**, 463
- Fynbo, J. P. U., et al. 2003, *A&A*, **406**, L63
- Galama, T. J., et al. 1998, *Nature*, **395**, 670
- Gallagher, J. S., Garnavich, P. M., Berlind, P., Challis, P., Jha, S., & Kirshner, R. P. 2005, *ApJ*, **634**, 210
- Gal-Yam, A., Ofek, E. O., & Shemmer, O. 2002, *MNRAS*, **332**, L73
- Garnavich, P., Jha, S., Kirshner, R., & Berlind, P. 1998, IAU Circ., 7066, 1
- Garnett, D. R. 2002, *ApJ*, **581**, 1019
- Garnett, D. R., Edmunds, M. G., Henry, R. B. C., Pagel, B. E. J., & Skillman, E. D. 2004a, *AJ*, **128**, 2772
- Garnett, D. R., Kennicutt, Jr., R. C., & Bresolin, F. 2004b, *ApJ*, **607**, L21
- Garnett, D. R., Shields, G. A., Skillman, E. D., Sagan, S. P., & Dufour, R. J. 1997, *ApJ*, **489**, 63
- Gorosabel, J., et al. 2005, *A&A*, **444**, 711
- Granlund, A., Conroy, P. G., Keller, S. C., Oates, A. P., Schmidt, B., Waterson, M. F., Kowald, E., & Dawson, M. I. 2006, in *Ground-based and Airborne Instrumentation for Astronomy*, Proc. SPIE, Vol. 6269, ed. I. S. McLean, & M. Iye
- Greene, J. E., & Ho, L. C. 2004, *ApJ*, **610**, 722
- Guetta, D., & Della Valle, M. 2007, *ApJL*, **657**, L73
- Guetta, D., Piran, T., & Waxman, R. E. 2005, *ApJ*, **619**, 412
- Hammer, F., Flores, H., Schaerer, D., Dessauges-Zavadsky, M., Le Floc'h, E., & Puech, M. 2006, *A&A*, **454**, 103
- Hamuy, M., Phillips, M., & Thomas-Osip, J. 2003, IAU Circ., 8088, 3
- Hao, L., et al. 2005, *AJ*, **129**, 1783
- Henry, R. B. C., & Worthey, G. 1999, *PASP*, **111**, 919
- Hirschi, R., Meynet, G., & Maeder, A. 2005, *A&A*, **443**, 581
- Hjorth, J., et al. 2003, *Nature*, **423**, 847
- Ho, L. C., ed. 2004, *Coevolution of Black Holes and Galaxies* (Cambridge: Cambridge Univ. Press)
- Horne, K. 1986, *PASP*, **98**, 609
- Hu, J. Y., Qiu, Y. L., Qiao, Q. Y., Wei, J. Y., & Filippenko, A. V. 1997a, IAU Circ., 6783, 1
- Hu, J. Y., et al. 1997b, IAU Circ., 6783, 1
- Hurley, K., et al. 2002, GRB Coordinates Net., **1252**, 1
- Iwamoto, K., et al. 1998, *Nature*, **395**, 672
- Iwamoto, K., et al. 2000, *ApJ*, **534**, 660
- Jones, D. H., Saunders, W., Read, M., & Colless, M. 2005, *Publ. Astron. Soc. Aust.*, **22**, 277
- Jones, D. H., et al. 2004, *MNRAS*, **355**, 747
- Kennicutt, R. C. 1998, *ARA&A*, **36**, 189
- Kewley, L. J., Brown, W. R., Geller, M. J., Kenyon, S. J., & Kurtz, M. J. 2007, *AJ*, **133**, 882
- Kewley, L. J., & Dopita, M. A. 2002, *ApJS*, **142**, 35
- Kewley, L. J., Geller, M. J., Jansen, R. A., & Dopita, M. A. 2002, *AJ*, **124**, 3135
- Kewley, L. J., Groves, B., Kauffmann, G., & Heckman, T. 2006, *MNRAS*, **372**, 961
- Kewley, L. J., Jansen, R. A., & Geller, M. J. 2005, *PASP*, **117**, 227
- Kinugasa, K., Kawakita, H., Ayani, K., Kawabata, T., & Yamaoka, H. 2002, IAU Circ., 7811, 1
- Kniazev, A. Y., Grebel, E. K., Hao, L., Strauss, M. A., Brinkmann, J., & Fukugita, M. 2003, *ApJ*, **593**, L73
- Kobulnicky, H. A., & Kewley, L. J. 2004, *ApJ*, **617**, 240
- Kobulnicky, H. A., & Skillman, E. D. 1997, *ApJ*, **489**, 636
- Langer, N., & Norman, C. A. 2006, *ApJ*, **638**, L63
- Lee, E., & Li, W. 2005, IAU Circ., 8570, 1
- Lee, N., & Li, W. 2007, *Central Bureau Electronic Telegrams*, ed. D. W. E. Green, **807**, 1
- Le Floc'h, E., et al. 2003, *A&A*, **400**, 499
- Leibundgut, B., Kirshner, R. P., Pinto, P. A., Rupen, M. P., Smith, R. C., Gunn, J. E., & Schneider, D. P. 1991, *ApJ*, **372**, 531
- Leonard, D. C., & Filippenko, A. V. 2005, in ASP Conf. Ser. 342: 1604–2004: Supernovae as Cosmological Lighthouses, ed. M. Turatto, S. Benetti, L. Zampieri, & W. Shea (San Francisco, CA: ASP), 330
- Lequeux, J., Peimbert, M., Rayo, J. F., Serrano, A., & Torres-Peimbert, S. 1979, *A&A*, **80**, 155
- Li, L.-X. 2006, *MNRAS*, **372**, 1357
- Li, W., Filippenko, A. V., Treffers, R. R., Riess, A. G., Hu, J., & Qiu, Y. 2001, *ApJ*, **546**, 734
- Liang, E., Zhang, B., Virgili, F., & Dai, Z. G. 2007, *ApJ*, **662**, 1111
- Maeda, K., Nomoto, K., Mazzali, P. A., & Deng, J. 2006, *ApJ*, **640**, 854
- Malesani, D., et al. 2004, *ApJ*, **609**, L5
- Mannucci, F., Della Valle, M., Panagia, N., Cappellaro, E., Cresci, G., Maiolino, R., Petrosian, A., & Turatto, M. 2005, *A&A*, **433**, 807
- Margutti, R., et al. 2007, *A&A*, **474**, 815
- Matheson, T., Filippenko, A. V., Li, W., Leonard, D. C., & Shields, J. C. 2001, *AJ*, **121**, 1648
- Matheson, T., et al. 2000, *AJ*, **120**, 1487
- Matheson, T., et al. 2003, *ApJ*, **599**, 394
- Matheson, T., et al. 2007, *AJ*, submitted
- Mazzali, P. A., et al. 2002, *ApJ*, **572**, L61
- Mazzali, P. A., et al. 2003, *ApJ*, **599**, L95
- Mazzali, P. A., et al. 2005, *Science*, **308**, 1284
- Mazzali, P. A., et al. 2006a, *Nature*, **442**, 1018
- Mazzali, P. A., et al. 2006b, *ApJ*, **645**, 1323
- McCall, M. L., Rybski, P. M., & Shields, G. A. 1985, *ApJS*, **57**, 1
- McGaugh, S. S. 1991, *ApJ*, **380**, 140
- Miller, J. S., & Mathews, W. G. 1972, *ApJ*, **172**, 593
- Mirabal, N., Halpern, J. P., An, D., Thorstensen, J. R., & Terndrup, D. M. 2006, *ApJ*, **643**, L99
- Modjaz, M. 2007, PhD thesis, AA (Harvard Univ.)
- Modjaz, M., Challis, P., Kirshner, R., Matheson, T., & Berlind, P. 2005, IAU Circ., 8575, 4
- Modjaz, M., Kirshner, R. P., & Challis, P. 2008, *ApJL*, submitted (arXiv: [0801.0221](https://arxiv.org/abs/0801.0221))
- Modjaz, M., Li, W., Filippenko, A. V., King, J. Y., Leonard, D. C., Matheson, T., Treffers, R. R., & Riess, A. G. 2001, *PASP*, **113**, 308
- Modjaz, M., et al. 2006, *ApJ*, **645**, L21
- Moustakas, J., & Kennicutt, Jr., R. C. 2006a, *ApJS*, **164**, 81
- Moustakas, J., & Kennicutt, Jr., R. C. 2006b, *ApJ*, **651**, 155
- Mulchaey, J., & Gladders, M. 2005, *LDSS-3 User's Guide* (Pasadena, CA: Carnegie Obs.) available at <http://www.lco.cl/lco/telescopes-information/magellan/instruments-1/lcss-3-1/>
- Nakano, S., Aoki, M., Jha, S., Challis, P., Garnavich, P., & Kirshner, R. 1997, IAU Circ., 6770, 2
- Nakano, S., Kushida, R., Kushida, Y., & Li, W. 2002, IAU Circ., 7810, 1
- Osterbrock, D. E. 1989, *Astrophysics of Gaseous Nebulae and Active Galaxies* (Mill Valley, CA: University Science Books)
- Pagal, B. E. J., Edmunds, M. G., Blackwell, D. E., Chun, M. S., & Smith, G. 1979, *MNRAS*, **189**, 95
- Patat, F., et al. 2001, *ApJ*, **555**, 900
- Pérez-Montero, E., & Díaz, A. I. 2003, *MNRAS*, **346**, 105
- Pettini, M., & Pagel, B. E. J. 2004, *MNRAS*, **348**, L59
- Pian, E., et al. 2006, *Nature*, **442**, 1011
- Pilyugin, L. S. 2001, *A&A*, **374**, 412
- Pinto, P. A. 2004, *Bull. Am. Astron. Soc.*, 1563
- Pooley, D., & Lewin, W. H. G. 2003, IAU Circ., **8110**, 2

- Prochaska, J. X., et al. 2004, *ApJ*, 611, 200
- Prochaska, J. X., Chen, H.-W., Dessauges-Zavadsky, M., & Bloom, J. S. 2007, *ApJ*, 666, 267
- Puckett, T., Sostero, G., Quimby, R., & Mondol, P. 2005, IAU Circ., 8639, 1
- Quimby, R. 2006, PhD thesis, AA (Univ. of Texas)
- Quimby, R., Mondol, P., Castro, F., Roman, B., & Rostopchin, S. 2006, IAU Circ., 8657, 1
- Rubin, V. C., Ford, Jr., W. K., & Whitmore, B. C. 1984, *ApJ*, 281, L21
- Savaglio, S., Glazebrook, K., & Le Borgne, D. 2006, in Am. Inst. Phys. Conf. Ser., ed. S. S. Holt, N. Gehrels, & J. A. Nousek (New York: AIP), 540–545
- Schlegel, D. J., Finkbeiner, D. P., & Davis, M. 1998, *ApJ*, 500, 525
- Schmidt, G. D., Weymann, R. J., & Foltz, C. B. 1989, *PASP*, 101, 713
- Schwartz, M. 1998, IAU Circ., 7065, 1
- Searle, L., & Sargent, W. L. W. 1972, *ApJ*, 173, 25
- Shi, F., Kong, X., Li, C., & Cheng, F. Z. 2005, *A&A*, 437, 849
- Skillman, E. D., Kennicutt, R. C., & Hodge, P. W. 1989, *ApJ*, 347, 875
- Smartt, S. J., Vreeswijk, P. M., Ramirez-Ruiz, E., Gilmore, G. F., Meikle, W. P. S., Ferguson, A. M. N., & Knapen, J. H. 2002, *ApJ*, 572, L147
- Soderberg, A. M. 2005, The Astronomer's Telegram, 671, 1
- Soderberg, A. M., Chevalier, R. A., Kulkarni, S. R., & Frail, D. A. 2006a, *ApJ*, 651, 1005
- Soderberg, A. M., & Kulkarni, S. R. 2005, The Astronomer's Telegram, 571, 1
- Soderberg, A. M., Kulkarni, S. R., Berger, E., & Frail, D. A. 2003, IAU Circ., 8087, 2
- Soderberg, A. M., Nakar, E., Berger, E., & Kulkarni, S. R. 2006b, *ApJ*, 638, 930
- Soderberg, A. M., et al. 2005, *ApJ*, 627, 877
- Soderberg, A. M., et al. 2006c, *Nature*, 442, 1014
- Sollerman, J., Östlin, G., Fynbo, J. P. U., Hjorth, J., Fruchter, A., & Pedersen, K. 2005, *New Astron.*, 11, 103
- Sollerman, J., et al. 2006, *A&A*, 454, 503
- Stanek, K. Z., et al. 2003, *ApJ*, 591, L17
- Stanek, K. Z., et al. 2006, *Acta Astron.*, 56, 333
- Stasińska, G. 2005, *A&A*, 434, 507
- Stoughton, C., et al. 2002, *AJ*, 123, 485
- Sutherland, R. S., & Dopita, M. A. 1993, *ApJS*, 88, 253
- Thoene, C. C., Greiner, J., Savaglio, S., & Jehin, E. 2007, *ApJ*, 671, 628
- Tonry, J., & Pan-STARRS Team. 2005, in Bull. Am. Astron. Soc., 1363
- Tremonti, C. A., et al. 2004, *ApJ*, 613, 898
- van den Bergh, S., Li, W., & Filippenko, A. V. 2005, *PASP*, 117, 773
- van Zee, L., Salzer, J. J., Haynes, M. P., O'Donoghue, A. A., & Balonek, T. J. 1998, *AJ*, 116, 2805
- Vink, J. S., & de Koter, A. 2005, *A&A*, 442, 587
- Wade, R. A., & Horne, K. 1988, *ApJ*, 324, 411
- Wang, L., & Wheeler, J. C. 1998, *ApJ*, 504, L87
- Wang, L., et al. 2002, *ApJ*, 579, 671
- Wiersema, K., et al. 2007, *A&A*, 464, 529
- Wolf, C., & Podsiadlowski, P. 2007, *MNRAS*, 375, 1049
- Woosley, S. E., & Bloom, J. S. 2006, *ARA&A*, 44, 507
- Woosley, S. E., & Heger, A. 2006, *ApJ*, 637, 914
- Woosley, S. E., Heger, A., & Weaver, T. A. 2002, *Rev. Mod. Phys.*, 74, 1015
- Woosley, S., & Janka, T. 2005, *Nature Phys.*, 1, 147
- Yoon, S.-C., & Langer, N. 2005, *A&A*, 443, 643
- York, D. G., et al. 2000, *AJ*, 120, 1579